

Review

# Gases in Food Production and Monitoring: Recent Advances in Target Chemiresistive Gas Sensors

Nagih M. Shaalan <sup>1,2,\*</sup> , Faheem Ahmed <sup>1</sup> , Osama Saber <sup>1,3</sup>  and Shalendra Kumar <sup>1,4</sup> <sup>1</sup> Department of Physics, College of Science, King Faisal University, Al-Ahsa 31982, Saudi Arabia<sup>2</sup> Physics Department, Faculty of Science, Assiut University, Assiut 71516, Egypt<sup>3</sup> Egyptian Petroleum Research Institute, Nasr City 11727, Egypt<sup>4</sup> Department of Physics, School of Engineering, University of Petroleum & Energy Studies, Dehradun 248007, India

\* Correspondence: nmohammed@kfu.edu.sa

**Abstract:** The rapid development of the human population has created demand for an increase in the production of food in various fields, such as vegetal, animal, aquaculture, and food processing. This causes an increment in the use of technology related to food production. An example of this technology is the use of gases in the many steps of food treatment, preservation, processing, and ripening. Additionally, gases are used across the value chain from production and packaging to storage and transportation in the food and beverage industry. Here, we focus on the long-standing and recent advances in gas-based food production. Although many studies have been conducted to identify chemicals and biological contaminants in foodstuffs, the use of gas sensors in food technology has a vital role. The development of sensors capable of detecting the presence of target gases such as ethylene (C<sub>2</sub>H<sub>4</sub>), ammonia (NH<sub>3</sub>), carbon dioxide (CO<sub>2</sub>), sulfur dioxide (SO<sub>2</sub>), and ethanol (C<sub>2</sub>H<sub>5</sub>OH) has received significant interest from researchers, as gases are not only used in food production but are also a vital indicator of the quality of food. Therefore, we also discuss the latest practical studies focused on these gases in terms of the sensor response, sensitivity, working temperatures, and limit of detection (LOD) to assess the relationship between the gases emitted from or used in foods and gas sensors. Greater interest has been given to heterostructured sensors working at low temperatures and flexible layers. Future perspectives on the use of sensing technology in food production and monitoring are eventually stated. We believe that this review article gathers valuable knowledge for researchers interested in food sciences and sensing development.

**Keywords:** gases in food; food quality; carbon monoxide; ethylene; oxygen; ammonia; carbon dioxide; ethanol; sulfur dioxide; gas sensor in food



**Citation:** Shaalan, N.M.; Ahmed, F.; Saber, O.; Kumar, S. Gases in Food Production and Monitoring: Recent Advances in Target Chemiresistive Gas Sensors. *Chemosensors* **2022**, *10*, 338. <https://doi.org/10.3390/chemosensors10080338>

Academic Editor: Nicole Jaffrezic-Renault

Received: 5 July 2022

Accepted: 12 August 2022

Published: 17 August 2022

**Publisher's Note:** MDPI stays neutral with regard to jurisdictional claims in published maps and institutional affiliations.



**Copyright:** © 2022 by the authors. Licensee MDPI, Basel, Switzerland. This article is an open access article distributed under the terms and conditions of the Creative Commons Attribution (CC BY) license (<https://creativecommons.org/licenses/by/4.0/>).

## 1. Introduction

Due to global population growth, technology has played a large role in food production as food needs become more demanding in societies. Concerns about the production of poor-quality foods have been linked to increased rates of death, disease, and human suffering, which places a greater economic burden on humanity [1–3]. To reduce waste, poisoning, and spoilage in food, great efforts have been made in the industrial sector [4]. Technology has developed and has economic importance and plays a vital role in the quality of foods. Therefore, it has become necessary for food production and the industry to undergo food quality assurance that complies with international food safety rules. Thus, the importance of food science and technology has increased in terms of publications that gained a high *h*-index over the last five years (2017–2021), which was recently indicated by the google metric [5], as shown in Figure 1. The *h5*-index is defined as the *h*-index for articles published in the last five complete years. It is the largest number *h*, such that *h* articles published in 2017–2021 have at least *h* citations each [6]. Food chemistry gained the highest *h5*-index with 122, followed by trends in food science and technology, and critical reviews in food

science and nutrition. Food control and food quality also have a high *h5*-index, with 77 and 66, respectively.

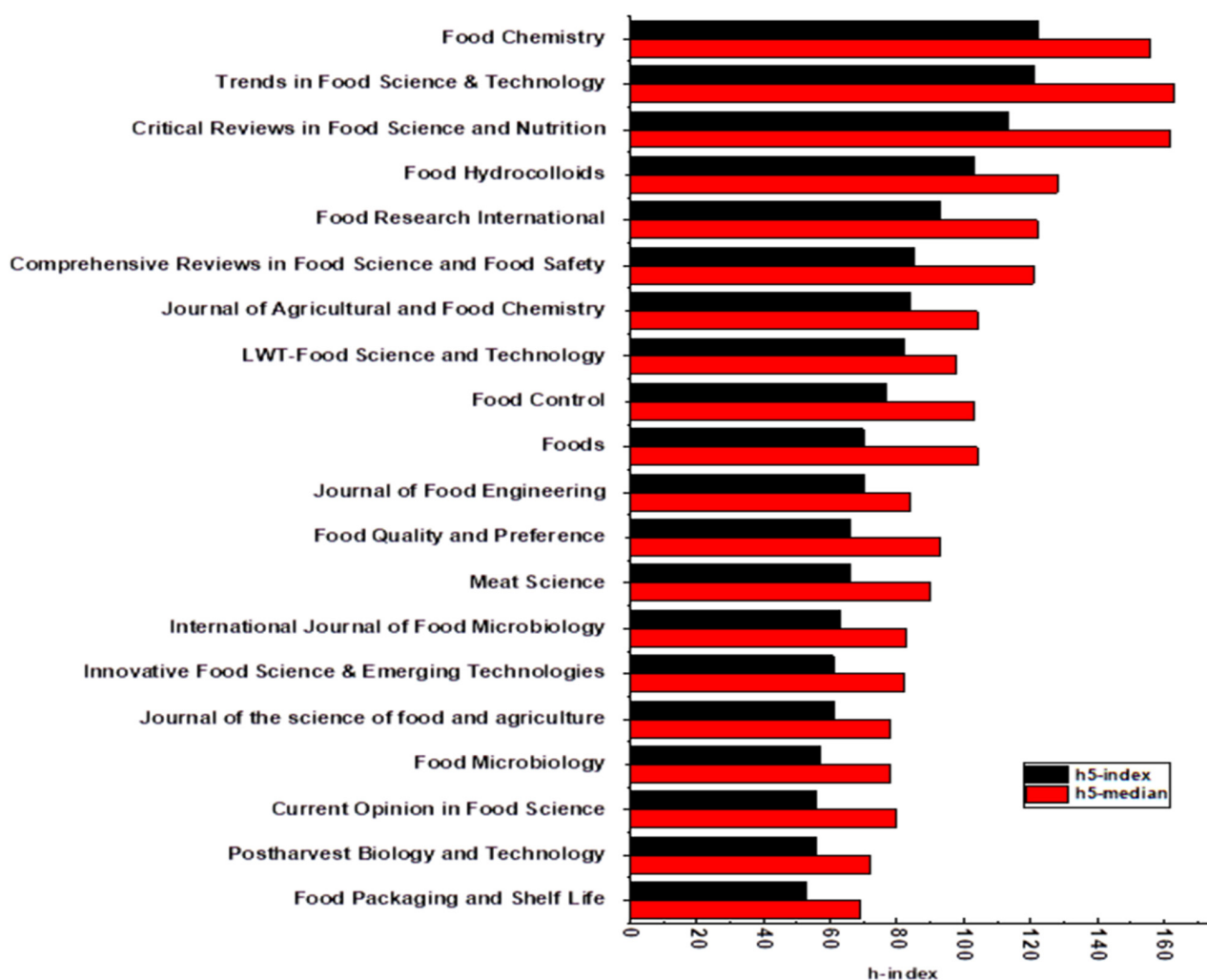


**Figure 1.** The *h5*-index for articles published in the last five complete years (2017–2021) in food science and technology.

The global gas sensors market was valued at \$2.50 billion in 2021. It is expected to expand at a compound annual growth rate (CAGR) of 8.9% from 2022 to 2030 [7]. The main factor driving the gas sensor market is the development of miniaturization and wireless capabilities, along with improvements in communication technologies that enable them to be integrated into various devices and machines to detect toxic gases at a safe distance. The CO<sub>2</sub> sensor segment dominated the market in 2021 and captured more than 31.0% of the global revenue share. CO<sub>2</sub> sensors are primarily used to monitor indoor air quality in homes, office buildings, automobiles, healthcare, agriculture, and other applications. The agricultural sector captured a share of about 10% of the global revenue of the gas sensing market in 2021. Agricultural gas sensors are used to monitor and detect hazardous gases used in food production and food quality control. Food and beverage producers and processors use and produce hazardous gases in many stages, including the processing of food, waste, and by-products and the preservation of food until it is opened. Essentially, gases are used at every step of the food chain, from field to fork. Gases are used in many sectors of the food industry, such as meat and fish [8], vegetables, fruits [9], bakeries [10], and wine and beer [11]. They are used in many applications such as hydrogenation processes for oils, carbonation processes for vegetables [12], food preservation processes, and packaging processes [13]. Gases are also used and produced during various beverage

manufacturing processes, as shown in Figure 2. Gases are byproducts of the processes of ripening and spoilage of foods such as meat [14], vegetables, and fruits [15,16]. Gases are used in the food industry, agriculture, and with animals [17]. In animal production, gases are used in anesthetic processes before the slaughter process or in oxygenation processes in aquatic organisms. In plant production, gases are produced and used in greenhouses to provide a suitable climate for the process of growth, maturation, and storage, and to control pests [18,19]. Figure 2 shows the emitted and used gases in different processes in food production. The type of gas differs according to the stage of the purpose of utilization.  $\text{SO}_2$  gas is used in drink production, such as Oenology and microalgae cultivation, which is wine and beer production.  $\text{CO}_2$  is the most utilized gas, and is used in different processes. It is used in the anesthesia of animals in large quantities, greenhouses, microalgae cultivation, modified atmospheric packaging (MAP), and food storage. Other important gases are emitted due to the spoilage of food, indicating low quality or bad food conditions. These gases are emitted due to changes in the microorganisms in food, such as  $\text{C}_2\text{H}_4$  and  $\text{C}_2\text{H}_5\text{OH}$  in fruit and vegetable ripening; nitrogen dioxide in microalgae; and  $\text{NH}_3$ , hydrogen sulfate, and some rare detectable gases in meat spoilage.

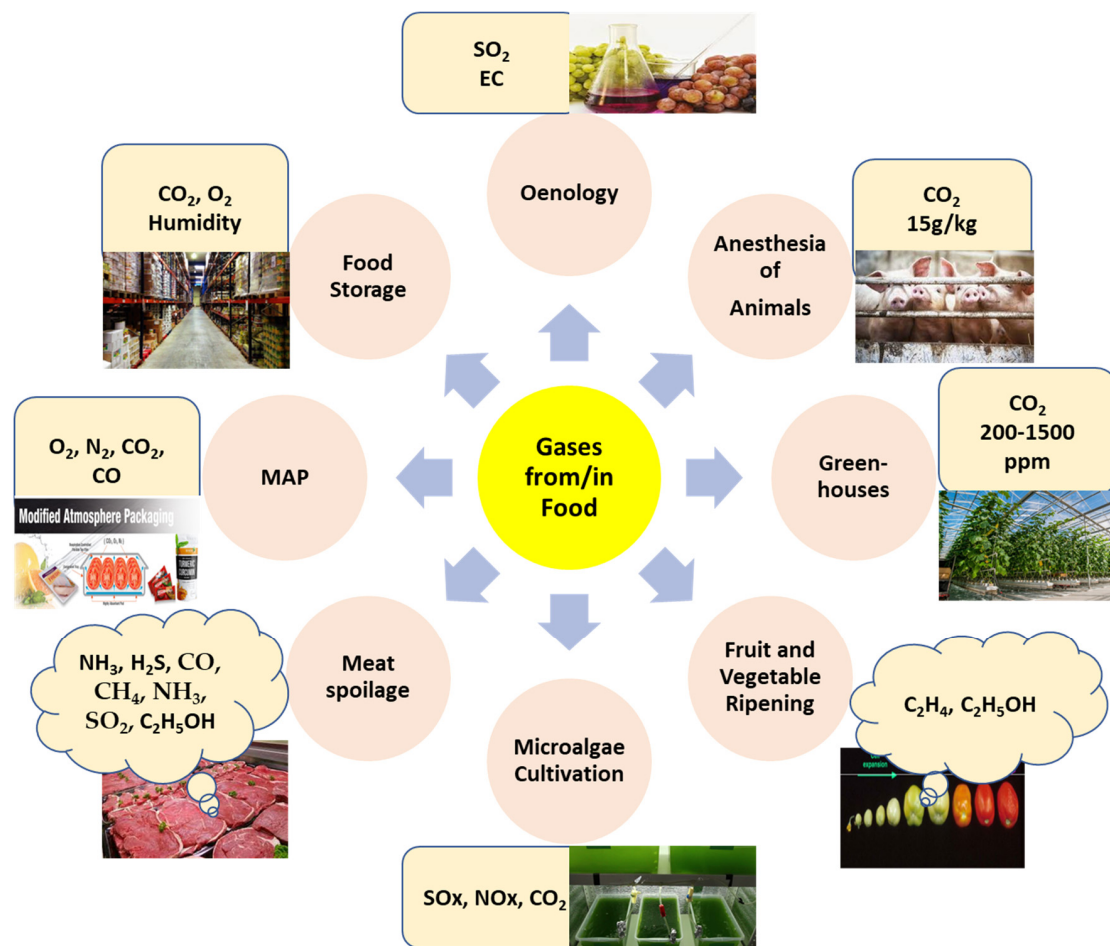


Figure 2. Scheme of the gases used in or produced from food operations.

One of the most important uses of gases is the process of preserving foods in packaging technology called modified atmospheric packaging (MAP), a technique used to preserve fresh or processed foods for long periods. In this technique, the air is replaced with other gases through which the chemical processes or oxidation reactions of enzymes can be slowed down, in addition to preventing the growth of pathogens and aerobic and anaerobic bacteria. Many foods are prepared in modified packages so that the food tastes and appears fresh for a long time without any modification of the food itself. The type of gas mixture

used depends on the target and the type of food. The MAP process is a common occurrence in food packaging. As a result, manufacturers have greater control over product quality, availability, and costs. They can eliminate product turnover, removal, and re-stocking, reducing costs and eliminating waste.

Gas sensors are necessary devices to accurately monitor and determine the concentrations of different gases when producing foods. The gas sensors used must be able to monitor and analyze the gas in real time. Thus, the sensors must provide high-accuracy and high-quality online sensing capabilities to detect the gases produced or used in food and beverages. Nanotechnology has changed many life applications, as nanomaterials have been applied in different fields because they have unique application properties. Nanomaterials prepared in various forms improve the properties of the materials and open new avenues for their application in industrial food. For example, nanomaterials, such as metal oxides [20], carbon nanotubes [15,21], and graphene, have been used in many chemical gas sensors to identify the existence of volatile organic compounds that are produced in food products owing to their spoilage and dangerous processes that may occur during the ripening, storage, and transportation of food [22–24].

In this review, our goal is to prepare an article on the most used or produced gases during the different stages of food production and monitoring, and the state of the art of chemiresistive sensor technology for the target gases. Thus, (1) we focus on the gases that have been consumed during oenology, animal production, greenhouse crops, modified atmospheric packaging, and microalgae cultivation. Additionally, attention is given to monitoring of food quality by detecting gases in meat spoilage, fruit and vegetable ripening, and humidity during food storage. (2) We focus on the most recent available sensors able to work under low temperatures and low levels of detection suitable for the real-time monitoring of gases during the various stages of the food chain.

## 2. Long-Standing and Recent Advances in Gas-Based Food Production

### 2.1. Gases in Drink Production

The fabrication of drinks needs to use some toxic gases, such as SO<sub>2</sub>, which has antioxidant properties [25]. This gas is toxic, heavier than air, stable under normal conditions, and corrosive of metals. However, it is critical for the production of wine, since it shields the wine from microbials and oxidation. It is added to prevent the unwanted development of microorganisms, as an antioxidant to inhibit polyphenol oxidases (laccase and tyrosinase), and as a dissolvent. SO<sub>2</sub> is also a food additive (E220) [26] that is commonly applied in the food industry. Oxidation processes negatively affect the organoleptic properties of the wine and lead to a loss of nutritional value. Phenols are the basis of the oxidation process, which causes enzymatic and non-enzymatic browning. Quinones are produced as by-products from the oxidation of phenol and hydrogen peroxide (H<sub>2</sub>O<sub>2</sub>), which is a strong oxidant. When SO<sub>2</sub> is used, it reduces quinones, inhibits oxidative enzymes, and reacts with H<sub>2</sub>O<sub>2</sub>. SO<sub>2</sub> works as an antimicrobial in the synthesized wine [27,28]. In addition to its main application in wine science, SO<sub>2</sub> is observed in dried fruits, meats, beer and fermented beverages, candied fruits, and jellies. Additionally, one of the most dangerous compounds is ethyl carbamate (EC). EC is a carcinogenic material that is commonly observed in alcoholic beverages [29]. Much research work has focused on this compound, which is considered a significant challenge that exists in the beverage industry.

### 2.2. Gases in Anesthesia of Animals

One of the methods used in the process of slaughtering animals is the use of CO<sub>2</sub> for stunning. This gas causes unconsciousness after inhalation of a CO<sub>2</sub>-based atmosphere mixed with air or nitrogen (N<sub>2</sub>), oxygen (O<sub>2</sub>), or argon (Ar) [17]. The use of gas in this process takes a few minutes because extremely high levels of CO<sub>2</sub> greater than 30% cause the animal to have conscious convulsions. Accordingly, the animal is exposed to CO<sub>2</sub>, the level of which is gradually increased until it reaches a maximum concentration level of 70% of CO<sub>2</sub> to create a severe stun [30]. To ensure the animal is exposed to different

concentrations of gas, the animal passes through a room in which the CO<sub>2</sub> content is increased continuously or passes through two rooms that contain different levels of gas, where the first has a limited concentration of CO<sub>2</sub> and the second has a high percentage of CO<sub>2</sub>. The consumption of CO<sub>2</sub> is based on some parameters such as weight. In the case of pigs, the value of CO<sub>2</sub> is about 100–500 g/pig. The specific CO<sub>2</sub> consumption of poultry depends on the equipment design and the breed and weight of the animal. In the case of chickens, the average value of CO<sub>2</sub> is about 15 g/kg [31].

### 2.3. Gases in Greenhouses

CO<sub>2</sub> has been used in commercial greenhouses for more than four decades, which is a byproduct of burning natural gas that is used to heat the greenhouses [32]. Farmers of vegetables, flowers, and plants use different methods and rates to enrich CO<sub>2</sub>. Greenhouses can use either compressed or liquid CO<sub>2</sub> depending on how much gas is needed. The compressed CO<sub>2</sub> is converted from a liquid to a gas and then released into the greenhouse. Farmers can also use CO<sub>2</sub> stoves or generators to fertilize CO<sub>2</sub>. Some farmers use self-produced CO<sub>2</sub> while others use industrial CO<sub>2</sub>. However, some farmers found that when they used two to three times more CO<sub>2</sub> than the existing outside level, they obtained higher yields of their crops. To date, day and night greenhouse heating management technology depends on the frequency of the situation. Photosynthesis is the use of light as an energy source for the manufacture of organic materials using CO<sub>2</sub> in the atmosphere and water, accompanied by the production of oxygen by the plant. CO<sub>2</sub> is absorbed by the plant at a concentration of 0.03% (300 ppm), and if the concentration drops to 120–150 ppm, this prevents the photosynthesis processes. In greenhouses, this minimum level can be attained in a few hours if the greenhouse contains a lot of plants. Thus, by introducing CO<sub>2</sub>, the required minimum can be restored. Additionally, the required level varies according to the cultivated species of plants. It was found that the growth rate can be increased by increasing the level of CO<sub>2</sub> in the greenhouse. Thus, CO<sub>2</sub> with a level of 200 to 1500 ppm ensures an increase in the yield in terms of the weight and number of crops [33–36]. It also supports faster growth, earlier harvest, stronger stems, better flower color quality, and healthy growth with disease resistance. Greenhouses are closed environments in which the conditions are optimized for plant growth. Optimal controls require information from both the indoor and outdoor environments. Typically, CO<sub>2</sub> is measured inside greenhouses. A CO<sub>2</sub> m is needed to both monitor CO<sub>2</sub> and control CO<sub>2</sub> enrichment in the greenhouse. Handheld, stationary, and computer-controlled sensors are available and vary in their level of sophistication and accuracy. To date, the greenhouse environment has been monitored and controlled using CO<sub>2</sub> sensors, usually an infrared gas analyzer (IRGA), to monitor the minimum and maximum CO<sub>2</sub> levels [37]. This is carried out by distributing more than one IRGA inside the greenhouse, which is controlled by sensors connected to a computer to control the environment. A metal oxide-sensitive layer is also used to monitor CO<sub>2</sub> [38].

### 2.4. Gases in Modified Atmospheric Packaging (MAP)

Many of the foods we consume such as fruits, vegetables, meats, and baked goods are packaged in a modified atmosphere to extend their shelf life [39]. The modified atmosphere ensures the food taste the same and looks fresher for longer without modifying the food itself [40]. Modified atmosphere packaging (MAP) is achieved by replacing the air around the food with a mixture of gases designed specifically for food items, where CO<sub>2</sub> may change from 20% to 100% [41]. MAP is often used in dairy, meat, poultry, seafood, dried fruit and vegetable, bakery, and medical applications. The MAP process lowers the volume of oxygen within the space of the packaging containing the product. Thus, the oxygen inside the package is often replaced with other gases. The gases that are most used in the packaging process are nitrogen, CO<sub>2</sub>, and oxygen. In some cases, argon and carbon monoxide are used to preserve the color of red meat in a low-oxygen atmosphere. The ambient air contains 78% N<sub>2</sub>, 21% O<sub>2</sub>, and 1% Ar, in addition to rare gases. O<sub>2</sub> gas must be carefully used because it may react with the food or provide conditions for the growth of



microorganisms, which leads to food spoilage. MAP is widely used because it provides a way to extend food life without the addition of any chemical additives or preservatives. For example, meat benefits from MAP containing 70–80% of O<sub>2</sub> while seafood needs a low level of O<sub>2</sub> and high levels of CO<sub>2</sub>. The concentration of CO<sub>2</sub> used varies according to the type of packaging, as loose packaging requires very high concentrations of CO<sub>2</sub>. The use of ideal gas compositions also differs between the storage of fish and meat due to the presence of myoglobin in meat, an iron-containing protein that has a purple color and can react with oxygen gas molecules to form oxymyoglobin, which has a red color associated with fresh meat. However, if it largely reacts with oxygen, it forms methemoglobin [42], which is the brown color associated with spoiled food. Thus, it depends on the concentration of oxygen in the surrounding atmosphere. Likewise, for cooked foods, an oxygen-free environment is ideal for preserving food, and CO<sub>2</sub> is the preferred gas in this case. The role of CO<sub>2</sub> is to exclude oxygen, which leads to deterioration of the state of food, unlike raw meat. In higher concentrations, CO<sub>2</sub> acts as an insecticide and protects products from pests. Cooked meat needs at least 30% CO<sub>2</sub> to preserve food for a longer period. Additionally, cheese, bakery products, fish, ready-made meals, and vegetables need a concentration of CO<sub>2</sub> up to 50%. In the case of plant foods, oxygen sometimes helps the plant to breathe. Therefore, balancing of the gas mixture between oxygen and CO<sub>2</sub> is important to slow the breathing process and maintain the freshness of food. Carbon monoxide (CO) is sometimes used in raw meat in a low-oxygen atmosphere. Carbon monoxide is similar to oxygen, as it reacts with myoglobin to form carboxymyoglobin, which gives it a cherry color. However, this gas has no taste, color, or odor, and it is poisonous. Carbon monoxide is a poisonous gas and in industry, it can indicate meat is fresh even if it is spoiled. It is dangerous.

### 2.5. Gases in Microalgae Cultivation

Microalgae selection criteria relate to the particular growth and high tolerance of strains of microalgae of flue gas, including elevated levels of CO<sub>2</sub>, SO<sub>x</sub>, and NO<sub>x</sub> [43]. In addition, these strains tolerate the high temperatures that usually accompany the flue gas supply. An appropriate strain should be chosen to be investigated or made. It is exciting to recover the bibliographic work with the initial cultivation experiments that can be achieved in a lab scale-photobioreactor. There are three modes of microalgae cultivation. The first is autotrophic, in which mineral compounds and light are used. The second is a heterotrophic mode, in which organic compounds such as glucose are used. The third is a nutrition mixture called mixotrophically, which is a mixture between the first and second modes. The first and second modes are related to the use of flue gases in agriculture. In this type of farming, in addition to controlling the use of light, the gas distribution, air quality, and mixing quality of the cultivation are also controlled. This is to carry out the process of transferring CO<sub>2</sub> as the main source of carbon and to avoid the deposition of microalgae cells. The bio-fixations of CO<sub>2</sub> by microalgae depend on the choice of the microalgae strains that are cultivated [44]. Microalgae use CO<sub>2</sub> to create and develop cells and ensure their metabolism. In some species of microalgae, optimum CO<sub>2</sub> removal occurs when the CO<sub>2</sub> level is reduced to 1%. The higher the CO<sub>2</sub> content, the higher the percentage of lipids and acids produced by the microalgae, which represents a clean environment and economic area of interest to humanity. The total lipids are 30% to 50% of the CO<sub>2</sub> level when the O<sub>2</sub> level is low, affecting enzymatic saturation. The removal of CO<sub>2</sub> depends on the microalgae species, cultivation system, temperature, CO<sub>2</sub> concentration, and growth rate. The control of the CO<sub>2</sub> concentration is an effective parameter in this type of cultivation; thus, the measurement of its level should be accurate. Flue gases must be known before they can be used in microalgae culture, as some untreated flue gases exhibit higher levels of SO<sub>x</sub>, CO<sub>2</sub>, and NO<sub>x</sub>. However, being aware of these components enables the selection of strains that are biologically resistant to the toxic gases and that offer a high growth rate. Without this, the cultural process may be inhibited and fail or die [45–47]. The more tolerant the breeds are of these toxic gases, the lower the cost of pre-culture gas treatment. The CO<sub>2</sub>,

SO<sub>x</sub>, and NO<sub>x</sub> concentrations for different strains' performance were 30–70%, 30–100 ppm, and 50–100 ppm, respectively [44].

### 2.6. Gases in Meat Spoilage

Meat spoilage is a metabolic process that alters the organoleptic properties of meat and is not acceptable for use or human consumption. If favorable conditions are provided for the spoilage process, such as increased humidity, low oxygen, and low temperatures, these are ideal conditions for the growth of microbes [48,49]. When microbes grow and damage meat, poultry, and fish products, volatile nitrogen-containing compounds are produced in large amounts. The blood circulation of the animal stops after the slaughter process, in addition to the respiratory system, so the meat undergoes the anaerobic glycolysis process, which lowers the pH, and autolysis of protein produces amino acids that make the meat vulnerable to microbial spoilage. This is followed by the formation of volatile compounds such as H<sub>2</sub>S and NH<sub>3</sub> gases, the most known compounds with a pungent odor [48]. Therefore, the concentrations of H<sub>2</sub>S and NH<sub>3</sub> are the main indicators used to determine the freshness of meat during storage periods. Therefore, measurement of these concentrations reflects the freshness of meat in the market [50]. There are a few other types of gases and volatiles produced by meat spoilage. For example, in fish spoilage, CO, CH<sub>4</sub>, SO<sub>2</sub>, alcohols, amines, and sulfurs are observed [51].

### 2.7. Gases in Fruit and Vegetable Ripening

Monitoring fresh fruits and vegetables after harvest is a very important matter. Therefore, the process of controlling the surrounding atmosphere must be carefully controlled [52,53]. Researchers found that fruits absorb oxygen and then produce CO<sub>2</sub>, and they found that fruits that were kept in an atmosphere that did not contain oxygen did not ripen. The implementation of commercial “controlled atmosphere” storage is widely used for many fresh fruits and vegetables in many countries. Extension of the shelf life of some types of fruits can be achieved in controlled weather for several months. This atmosphere slows maturation and maintains firmness, causing a delay in the development of the flavor while the sweetness and texture can be maintained to an extent. This is carried out by reducing the oxygen in an airtight storage room, thus reducing the respiration of the fruit. Ordinary air contains 21% oxygen, which is reduced to 1–3% by pumping nitrogen gas into closed rooms. The optimum levels of O<sub>2</sub>, CO<sub>2</sub>, and C<sub>2</sub>H<sub>4</sub> vary between fruits and vegetables and even between varieties and production areas [54]. However, the high level of the CO<sub>2</sub> concentration in the store leads to spoilage of the fruit and vegetables. Additionally, if the level of oxygen is decreased, the respiration of fruits changes from aerobic to fermentation, which results in volatile substances such as ethyl acetate, acetaldehyde, and C<sub>2</sub>H<sub>5</sub>OH. This shows us C<sub>2</sub>H<sub>5</sub>OH gas can be collected and measured to monitor the state of fermentation that has just begun, and accordingly, the oxygen level can be increased to prevent the spoilage of fruits.

C<sub>2</sub>H<sub>4</sub> gas is an unsaturated hydrocarbon molecule, produced in most fruits, and it is the ripening hormone in fruit [16]. The level of C<sub>2</sub>H<sub>4</sub> gas varies according to the state of ripening of the fruits. Thus, it is at a very low level in the case of immature fruits and increases with the growth of the fruits as large quantities are produced, causing an increase in the ripening process until it reaches the peak and then the production of C<sub>2</sub>H<sub>4</sub> begins to decrease again due to the beginning of spoilage [16]. The level of C<sub>2</sub>H<sub>4</sub> also varies according to the type of fruit. If large quantities of C<sub>2</sub>H<sub>4</sub> are produced from fruits, it is difficult to store them once this happens. For example, the McIntosh apple fruit produces huge quantities of C<sub>2</sub>H<sub>4</sub>. Therefore, the harvesting process must take place before the C<sub>2</sub>H<sub>4</sub> level begins to increase rapidly in the case of months of storage.

Peaches and plums are very sensitive to C<sub>2</sub>H<sub>4</sub> hormone, so they ripen quickly after being harvested [55]. However, some types of fruits can be stored for longer periods if the C<sub>2</sub>H<sub>4</sub> production process is suppressed. Moreover, the adaptability and performance of crops are also affected by C<sub>2</sub>H<sub>4</sub> under stress conditions. Controlled atmosphere storage

tests at  $C_2H_4$  concentrations ranging from 0.001 to 10 ppm have proven successful in prolonging the storage life of commercial products for several weeks depending on the species [56,57].  $C_2H_4$  is harmful to stored fruit and vegetables but is useful in other cases. Some fruits are harvested in an early state and the greenery remains in these fruits. These fruits (especially bananas) are placed in ripening rooms and exposed to  $C_2H_4$  gas.  $C_2H_4$  can be used in the form of liquids, such as ethyl, to produce  $C_2H_4$  when sprayed on the fruit.  $C_2H_4$  is also used in gaseous form, with a ratio of 5% to 95% of nitrogen.

### 3. Recent Advances in Target Gas Sensing

Although many studies have been conducted to identify the chemical and biological contaminants in foodstuffs, the use of gas sensors in food technology plays a vital role. The development of sensors capable of detecting the presence of gases such as  $C_2H_4$ ,  $NH_3$ ,  $CO_2$ ,  $SO_2$ , and  $C_2H_5OH$  has been the target of study of many researchers, as gases are not only used in food production but are also a vital indicator of the quality of food. Therefore, in this section, we will discuss the latest practical articles that deal with these gases and their response, sensitivity, working temperatures, and limit of detection (LOD). We attempt to focus on the most recent research work, especially for sensors working in low temperatures and flexible sensors, if any.

#### 3.1. Recent Advances in $C_2H_4$ Gas Sensors

The process of measuring the percentage of  $C_2H_4$  is complicated and expensive because it uses advanced laboratory equipment to detect the presence of  $C_2H_4$  to determine whether the fruits are storable or not. In the distribution chains of fruits, it is necessary to control ripening through the level of  $C_2H_4$  to evaluate the fruit quality in the markets. Recently, the literature has concentrated on the detection of the ripening of agricultural products to avoid food waste by controlling  $C_2H_4$  [58–60]. Xiao et al. [16] reported a significant study on important ripeness restrictions depending on  $C_2H_4$  production in bananas in case of natural ripeness. They reported that  $C_2H_4$  production in natural ripening fruits increased drastically after day 15 of green banana storage, reached the highest production on day 18, and then decreased. The lowest concentration of  $C_2H_4$  depends on the ripening days and amount of food, such as fruits or vegetables. Banana produces 1.5  $\mu L/kg$  of  $C_2H_4$  gas, as a maximum value, for natural ripening. However, the production of  $C_2H_4$  depends on the ripening stage of the fruits. The  $C_2H_4$  concentration ranges from 0.5  $\mu L/kg$  (0.5 ppm/kg) on the first day of ripening and then increases up to 1.5  $\mu L/kg$  (1.5 ppm/kg) as the maximum ripening stage before spoilage. Thus, the detection of  $C_2H_4$  at a value lower than 0.5 ppm is required for early detection. Chemiresistive sensors are promising due to their low cost and easy integration. However, the challenge for these sensors is still working in high temperatures. Thus, development is ongoing in terms of obtaining a high-performance  $C_2H_4$  sensor. Recently, an  $C_2H_4$  sensor was fabricated based on a palladium-loaded tin oxide sensor to assess fruit quality [61]. The sensor showed an optimal performance with a response of 11 toward an  $C_2H_4$  concentration of 100 ppm at a high temperature of 250 °C, although its LOD was 50 ppb with good stability. Fong et al. [58] designed a novel sensor for  $C_2H_4$  built with doped CNTs and based on a mechanism called Wacker oxidation. This mechanism is based on the incorporation of a noble metal catalyst such as palladium to add oxygen to the  $C_2H_4$  molecule with an oxidation process. Additionally, Shaalan et al. [15,21] developed an  $C_2H_4$  gas sensor based on the defect-induced MWCNTs. These defect-induced CNTs were produced using Ni/Cr as catalyst layers in the PECVD system. They assessed the sensor at room temperature (RT) in a low  $C_2H_4$  concentration of 130 to 10 ppm. The sensor can also monitor natural fruits' ripeness at various stages in terms of its measurement accuracy, reliability, and reproducibility. The sensor can detect  $C_2H_4$  released from a single banana, as shown in Figure 3. Figure 3a exhibits the measured sensor response over five days of monitoring of bananas. Figure 3b shows the sensor signal corresponding to the ripening level observed in Figure 3c. More recent attempts toward  $C_2H_4$  are recorded in Table 1 for the most recent



literature. As reported in [16], the emitted amount of  $C_2H_4$  depends on the ripening day, where the level of  $C_2H_4$  increases with the ripening days, reaching the highest ripening level, and then decreases at the start of the spoilage stage. As shown in Figure 3, the as-received banana has a whitish green color, which shows a low peak of the sensor signal. On the second and third days of the experiment, the color changes from green to yellow, which gives a higher sensor signal. It is observed that on the fourth day, the dark color appears on the banana surface and increases by the fifth day, and, again, a low signal is detected compared to the third day due to the start of the spoilage.

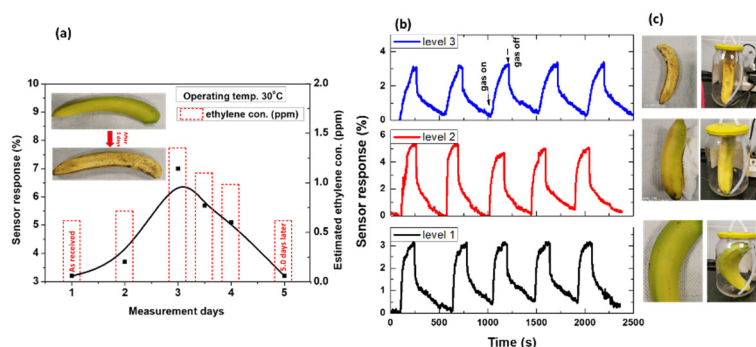


**Figure 3.** (a) Sensor response of a single banana as a function of the ripening days, detecting the ripening of banana over five days; (b) Repeated sensor signal (five cycles) for (c) different bananas at different ripening levels. Figures adapted with permission from [21].

**Table 1.** The most recent chemiresistive  $C_2H_4$  sensors reported in the literature.

Materials	Operating Temp. ( $^{\circ}C$ )	$C_2H_4$ Concentration	Response %	Limit of Detection	Ref.
Defective-CNTs	RT	300 ppb	~2.7	130 ppb	[15,21]
TiO <sub>2</sub> -WO <sub>3</sub>	250	100 ppm	1.2	8.0 ppm	[60]
Pd-SnO <sub>2</sub>	250	100 ppm	11.1	50 ppb	[61]
PANI/MWCNTs/SnO <sub>2</sub>	RT	100 ppm	1.2	10 ppm	[62]
Pd/rGO/ $\alpha$ -Fe <sub>2</sub> O <sub>3</sub>	250	1000 ppm	160	10 ppb	[63]
SnO <sub>2</sub>	375	2.5 ppm	15	—	[64]
Cr <sub>2</sub> O <sub>3</sub> -SnO <sub>2</sub>	350	2.5 ppm	17	—	
$\beta$ -MnO <sub>2</sub>	250	25 ppm	10.0	10 ppm	[65]
ZnO-Ag <sub>0.6</sub>	RT	30 ppm	5.6	—	[66]

### 3.2. Recent Advances in NH<sub>3</sub> Gas Sensors

According to the German Environment Agency, agriculture is the main source of NH<sub>3</sub> emissions, accounting for 95%. The pollutant NH<sub>3</sub> is mainly produced in animal husbandry because the excrements of farm animals contain urea and protein, which are converted into NH<sub>3</sub>. Additionally, NH<sub>3</sub> is a toxic and harmful gas, and it is one of the compounds produced due to the spoilage of meat and fish. It must be monitored in environments in which meat and fish is stored in stores or warehouses. To develop signs of spoilage in meat, the NH<sub>3</sub> concentration must be relatively high (>15 ppm) and/or the exposure time relatively long (>120 min) [67]. There are some cases where it is difficult to tell if meat has spoiled by detecting NH<sub>3</sub>, especially after the frozen storage period. However, contamination with low levels of NH<sub>3</sub> would greatly speed up the development of the rancid flavor. Therefore, there is a need to detect NH<sub>3</sub> at low concentrations and at RT to monitor food quality. Many efforts have been committed to developing high-performance sensors that are able to detect a low limit, and this challenge still faces many difficulties, especially those related to chemiresistive sensors in terms of the low operating temperature, response, and selectivity. A highly sensitive and flexible NH<sub>3</sub> sensor was fabricated from polyaniline/SrGe<sub>4</sub>O<sub>9</sub> (PSN) nanocomposite [68]. They reported that when the PSN sensor was subjected to 0.2 to 10 ppm at 25  $^{\circ}C$  and 60% RH, it exhibited

a significant response of 20.59% each 1.0 ppm. The sensor response of PSN was twice that of pristine PANI. In addition to its flexibility, the PSN sensor showed repeatability, stability, and selectivity to NH<sub>3</sub> at RT. Thus, this sensor has provided a very low NH<sub>3</sub> detection limit. Recently, promising chemical sensors for NH<sub>3</sub> have been developed for food spoilage monitoring based on organic field-effect transistors (OFETs) [69,70]. These OFET gas sensors were fabricated using solution-processable techniques and operated at low voltages. They provided a reliable sensing performance over multiple cycles of NH<sub>3</sub> exposure (2 to 50 ppm), with an estimated detection limit of less than 1 ppm and 2.17 ppb. Li et al. [71] studied CeO<sub>2</sub> nanoparticles annealed at a high temperature, which demonstrated good sensing toward NH<sub>3</sub>. The sensor response was about 25 and the response and recovery times were 3 and 116 s. It also offers reliable selectivity toward NH<sub>3</sub> and repeatability in the range of 0.5 to 1000 ppm. Recently, many good attempts at the detection of NH<sub>3</sub> using electrochemical sensing technology were carried out between 2017 and 2022. Some are shown in Table 2. Andre et al. [72] reported hybrid layer-by-layer films combined with polyaniline (PANI)-graphene oxide (GO)-zinc oxide ZnO for NH<sub>3</sub> sensing. They found that the films with tri-layers were the most adequate for sensing NH<sub>3</sub> in the range of 25 to 500 ppm. The prepared films were operated at RT and their response time was about 30 s. Lee et al. [73] developed a GO composite of Ti<sub>3</sub>C<sub>2</sub>T<sub>x</sub>/MXene layers. The MXene/rGO hybrid showed a significant improvement in the performance of the NH<sub>3</sub> response with low power consumption. The flexible structure of this composite also withstood the bending stress test. Accordingly, they sewed highly elastic MXene/rGO hybrid mixes into a lab coat using simple conventional weaving, showing a reliable sensing capability. Wearable sensors are of great importance due to their ability to monitor the workplace in real time. Therefore, the applications of wearable sensors in various fields have motivated researchers to develop the most reliable and efficient sensors. Wearable sensors are mainly based on flexible sensors that withstand mechanical deformations during use. For more about the development of these sensors based on two-dimensional materials, some of them have been monitored in [74]. We believe that this type of sensor creates a new path in the use of such sensors in the clothes of workers in markets and storage of meat, as such sensors provide quick results for determining whether that the products are in good condition or beginning to spoil.

**Table 2.** The most recent chemiresistive NH<sub>3</sub> sensors reported in the literature.

Materials	Operating Temp. (°C)	NH <sub>3</sub> Concentration	Response %	Limit of Detection	Ref.
PANI/SrGe <sub>4</sub> O <sub>2</sub>	RT	200 ppb	16.0	250 ppt	[68]
DPPT-TT-based	RT	2 ppm	~8.0	500 ppb	[69,70]
OFETs-based sensors		21 ppb	~22	2.17 ppb	
CeO <sub>2</sub>	RT	500 ppm	25	500 ppb	[71]
PANI/GO/PANI/ZnO	RT	100 ppm	38.3	23 ppm	[72]
MXene/rGO	RT	100 ppm	7.0	—	[73]
Carbon doped-TiO <sub>2</sub>	RT	100 ppm	18	—	[75]
Black phosphorus (BP)	RT	100 ppm	1.2	100 ppb	[76]
Ce-TiO <sub>2</sub>	RT	20 ppm	23.9	140 ppb	[77]
TiO <sub>2</sub> Nanospheres	250	300 ppm	2.1	—	[78]
N-TiO <sub>2</sub>	RT	3 ppm	1.2	1.0 ppm	[79]
TiO <sub>2</sub> /Ti <sub>3</sub> C <sub>2</sub> T <sub>x</sub>	RT	10 ppm	1.03	500 ppb	[80]

### 3.3. Recent Advances in SO<sub>2</sub> Gas Sensors

Sulphites can harm drinks' sensory properties, delay the onset of malolactic fermentation, and cause some health concerns in case of high concentrations in the final drinks. Thus, the SO<sub>2</sub> level in drinks is regulated, and it must be displayed on the label when found above 10 ppm or 10 mg/L [81]. Consequently, it is important in the drink-making process to control and manage the SO<sub>2</sub> content to maintain the lowest possible concentration while preserving its interesting properties. The recommended airborne exposure limit (REL) is

2 ppm over 10 h or 5 ppm for 5 min at a maximum [82]. Thus, several attempts have been made to detect SO<sub>2</sub> using various heterostructures to achieve a reliable and stable sensing layer at low temperatures (Table 3). Liu et al. [83] recently reported an ultra-sensitive sensor based on the use of nickel atoms attached to SnO<sub>2</sub> nanorods (SAC-Ni/H-SnO<sub>2</sub>), which are oxygen-rich vacancy sensing materials. The sensor response was 48 toward 20 ppm of SO<sub>2</sub> gas with a detection limit of 100 ppb. The sensing layer was characterized by DRIFTS and ESR, which demonstrate the coupling effects of SAC-Ni and adjacent oxygen vacancy on the surface of SnO<sub>2</sub> to enhance SO<sub>2</sub> uptake and the activation of chemically adsorbed oxygen as well. This efficient monoatomic catalyst provides innovative insight into the complex gas sensing layer. It also demonstrates a promising approach to using the monoatomic effect in sensing applications. However, the optimal operating temperature is still as high as 250 °C. Shinde et al. [84] developed a nano-hybrid sensing layer with a high response of 61.5% at 150 °C. This nano-hybrid layer was based on zinc–chromium hydroxide (ZC-LDH) and hexapotassium (HNb) nanosheets (ZCNb nanohybrids). The results clearly show that the lattice-designed 2D ZCNb nano-hybrids are very effective at not only improving the gas sensor activity but also in developing a new type of closely coupled LDH metal oxide-based hybrid material.

It is advantageous that micro-electromechanical systems (MEMSs) are used in gas sensor design, which may increase the accuracy and sensitivity of the sensors [85]. An MEMS was used to test low concentrations of SO<sub>2</sub> with SnO<sub>2</sub> layers and the heterogeneous structure of double NiO/SnO<sub>2</sub>. The sensing result confirmed that the NiO/SnO<sub>2</sub> sensing layer has better sensing properties than the single-SnO<sub>2</sub> layer because of the *p-n* junction formation. The NiO/SnO<sub>2</sub> sensing layer had the highest response of 20% at 400 ppb of SO<sub>2</sub> concentration, and 30% at 2000 ppb. The sensor works at a high temperature of 250 °C, although it shows selectivity towards SO<sub>2</sub> gas. Another study was conducted on the use of MEMSs in sensor design. Au nanoparticles with a diameter of about 5 nm were loaded onto the surfaces of La<sub>2</sub>O<sub>3</sub>-NPs, which were integrated by the MEMS into an Au/La<sub>2</sub>O<sub>3</sub>-NPs/ZnO/MEMS sensor [86]. In the presence of SO<sub>2</sub> gas at a concentration of 300 ppb, the Au/La<sub>2</sub>O<sub>3</sub>-NPs/ZnO/MEMS sensor displayed a higher response than the ZnO/MEMS or La<sub>2</sub>O<sub>3</sub>-NPs/MEMS sensors. The sensor was more sensitive to SO<sub>2</sub> than the other tested gases. However, it was operating at a temperature of 260 °C.

In a study investigating a ternary compound La<sub>1-x</sub>Ca<sub>x</sub>FeO<sub>3</sub> to low SO<sub>2</sub> concentrations, the La<sub>0.6</sub>Ca<sub>0.4</sub>FeO<sub>3</sub> thin film showed an excellent sensing performance [87]. It was found that La<sub>0.6</sub>Ca<sub>0.4</sub>FeO<sub>3</sub> displayed the best gas sensing performance, with a sensor response of 7.6 at an SO<sub>2</sub> concentration of 3 ppm at a low working temperature of 120 °C. The thin film was made using the DC-sputtering technique. The sensor showed a preferential selectivity for the detection of SO<sub>2</sub> gas under the operating condition compared to CH<sub>4</sub>, CO<sub>2</sub>, and CO. An MWCNT/MoS<sub>2</sub> nanocomposite prepared via a simple chemical method was proposed as a low-energy and RT operating sensor layer [88]. The device is selective towards SO<sub>2</sub> gas. A systematic examination of gas sensing using this film indicates a response of 0.22–1.81% in the concentration range of 500 ppb–3 ppm. The sensor was operating at RT and had a low bias voltage of 100 mV. The LOD level of the sensor was 500 ppb. We end this section with an important monograph, in which Zhai et al. presented a strategy for MOF sensor fabrication, describing a strategy for the development of a flexible sensor layer of UiO-66-NH<sub>2</sub> nanofiber through electrospinning and aqueous manufacture [89]. The sensor has high porosity and good flexibility; therefore, the sensor generated by the UiO-66-NH<sub>2</sub> nanofibers membrane combined with carbon nanotubes displayed a great response and stability to SO<sub>2</sub> for a gas concentration of 125 to 1.0 ppm at RT. The sensor showed selectivity towards SO<sub>2</sub> compared to other hazardous gases.

**Table 3.** The most recent chemiresistive SO<sub>2</sub> sensors reported in the literature.

Materials	Operating Temp. (°C)	SO <sub>2</sub> Concentration	Response %	Limit of Detection	Ref.
SAC-Ni/H-SnO <sub>2</sub>	250	20 ppm	48	100 ppb	[83]
ZCNb nanohybrids	150	100 ppm	61.5	100 ppb	[84]
MWCNT/MoS <sub>2</sub>	RT	1.0 ppm	1.9	500 ppb	[88]
NiO/SnO <sub>2</sub>	250	2.0 ppm	30	400 ppb	[85]
La <sub>0.6</sub> Ca <sub>0.4</sub> FeO <sub>3</sub> thin film	160	3.0 ppm	7.6	–	[87]
Au/La <sub>2</sub> O <sub>3</sub> -NPs/ZnO	260	1.0 ppm	44	100 ppb	[86]
PAN@UiO-66-NH <sub>2</sub>	RT	100 ppm	225	1.0 ppm	[89]
Ni-MOF/-OH-SWNTs	RT	1.5 ppm	28	1.0 ppm	[90]
PVF/TiO <sub>2</sub> nanocomposites	150	600 ppm	83	50 ppm	[91]

### 3.4. Recent Advances in CO<sub>2</sub> Gas Sensors

Artificial CO<sub>2</sub> is widely used in the food production process, especially in greenhouses, and the food preservation process. As we mentioned in Section 2.3, artificial fertilization of CO<sub>2</sub> is among the most common ways used to improve the environment in greenhouse applications for growth processes. The concentration levels of CO<sub>2</sub> are maintained at between 200 and 1500 ppm by CO<sub>2</sub> injection systems to optimize the growing conditions. If the level exceeds a concentration of 1500 ppm, it obstructs the productivity of the crops [33–36]. Thus, a sensing material should be sensitive of these CO<sub>2</sub> levels to be suitable for this application.

Various materials have been fabricated as sensing layers of CO<sub>2</sub> gas (Table 4). Recently, Thomas et al. [92] reported a high-performance sensor for CO<sub>2</sub>. The sensor was built from a porous *p*-Si/MoO<sub>3</sub> nanohybrid structure, which was synthesized through vacuum thermal evaporation on a microporous silicon substrate. The sensor presented an outstanding performance with a sensitivity of 15% for 150 ppm. It showed repeatability and a fast response of 8.0 s for 100 ppm at a high temperature of 250 °C. It was operated at a low temperature of 150 °C and a lower detection limit of 50 ppm. Bag and Pal [93] presented a polymer composite sensor functionalized with MWCNTs. The sensors were tested in different humidity conditions, showing a good performance. It showed the highest sensitivities from 500–5000 ppm under various relative humidity levels of 30 to 70% RH at RT. The fabrication of the sensing layer in an *n*-PSi/*p*-CuO/*n*-Cu<sub>2</sub>O bilayer heterostructure might be promising for CO<sub>2</sub> gas sensing [94]. The fabricated sensing layer was characterized at RT, showing sensitivity and reproducibility behavior. Additionally, the hybrid of CuO/rGO is intended for CO<sub>2</sub> sensing at RT [95]. The presence of multifunctional groups in the CuO/rGO hybrid and the high surface area created a highly sensitive sensing layer for CO<sub>2</sub> at RT. The thin layer of the CuO/rGO hybrid demonstrated a twice-sensing response compared to the rGO-based sensor for CO<sub>2</sub>. Additionally, the manufacture of sensors from hybrid materials is constantly increasing, for example, SnO<sub>2</sub> with reduced graphene oxide (rGO) together in a sensing layer to detect CO<sub>2</sub> at RT [96]. Due to the harmonious effect of mixing the near conductivity of metallic rGO and SnO<sub>2</sub>, the sensor showed an enhancement in the detection limit of 5 ppm of CO<sub>2</sub>. Moreover, it showed excellent sensing at RT and a humidity level of 58% RH. The sensor response was recorded, with a value of 1.206 toward 100 ppm of CO<sub>2</sub>, which was 6 times higher than the pure rGO sensing layer. The ternary hybrid sensing layer of rGO/NiO-In<sub>2</sub>O<sub>3</sub> displayed a good sensing performance when exposed to 5 ppm CO<sub>2</sub>, with quick response/recovery times of 6/5s at RT and an LOD of 5 ppm [97].

Mixing organic and inorganic materials appears to be fruitful in responding to gases, and this field is supposed to provide an opportunity for the manufacture of hybrid material-based electronic devices for sensing applications. Nasirian et al. [98] prepared a polyaniline/SnO<sub>2</sub> nanocomposite (PSN) sensor with various SnO<sub>2</sub> concentrations. They built a good sensor for the detection of CO<sub>2</sub> at RT. It showed a 39.2% response to about 5000 ppm CO<sub>2</sub>. Furthermore, the sensor exhibited reproducibility, reliability, and a selective response over multiple cycles for different CO<sub>2</sub> levels. In another study, sensors containing stacked layers of LaNiSbWO<sub>4</sub>-G-PPy (G: graphene, PPy: polymer polypyrrole) were fabricated [99]. The gas sensor showed a high response to CO<sub>2</sub> gas in the range of 200 to 4000 ppm at RT. It also showed a high selectivity. This gas sensor provided reproducibility, repeatability, and measurement accuracy. Continuing with the hybrid materials, a composite of multi-walled carbon nanotubes (MWCNTs) and a polypyrrolytic polymer (PPY) was synthesized as a sensing material [100]. The sensor displayed a response of 7.2 at a CO<sub>2</sub> concentration of 1000 ppm. The response and recovery times were 30 and 37 s at 250 ppm, respectively. In general, the sensing mechanism of CO<sub>2</sub> on the surface of the sensing layer mostly depends on the availability of highly reactive oxygen species. O<sub>2</sub> molecules are adsorbed on the sensing layer surface, forming O<sup>-</sup> species, which are reported to be highly reactive. Species of O<sup>-</sup> are considered to affect the adsorption process and react with the CO<sub>2</sub> molecules in the following processes [101]:



**Table 4.** The most recent chemiresistive CO<sub>3</sub> sensors reported in the literature.

Materials	Operating Temp. (°C)	CO <sub>2</sub> Concentration	Response %	Limit of Detection	Ref.
<i>p</i> -Si/MoO <sub>3</sub>	250	150 ppm	12.0	50 ppm	[92]
Sulfonated polyether ether ketone	RT	5000 ppm	47	500 ppm	[93]
CuO/rGO hybrid	RT	500 ppm	450	–	[95]
SnO <sub>2</sub> -rGO Hybrid	RT	500 ppm	4.5	10 ppm	[96]
rGO/NiO(8)-In <sub>2</sub> O <sub>3</sub>	RT	50 ppm	40	5 ppm	[97]
PANI-SnO <sub>2</sub> -UV	RT	5000 ppm	47.4	3000 ppm	[98]
G-LaNiSbWO <sub>4</sub> -PPy	RT	1800 ppm	120	400 ppm	[99]
MWCNT/PPY	RT	1000 ppm	7.2	250 ppm	[100]
PDDA- MWCNTs	RT	20 ppm	4.0	–	[102]
Au/PAni nanocomposites	RT	4000 ppm	2.0	–	[103]

### 3.5. Recent Advances in C<sub>2</sub>H<sub>5</sub>OH Gas Sensors

The level of C<sub>2</sub>H<sub>5</sub>OH released due to spoilage of fruits or vegetables depends on the amount and level of fermentation. C<sub>2</sub>H<sub>5</sub>OH is a naturally occurring substance resulting from the fermentation of fruit sugars by yeast. Fruits and vegetables are more susceptible to spoilage than grains due to their nature and composition. In this regard, Satish Babu [104] attempted to produce C<sub>2</sub>H<sub>5</sub>OH from vegetables rich in spoiled starch such as wild potatoes and sweet potatoes, which contain abundant starch. In the presence of enzyme-mediated amylase- and polysaccharide-producing microorganisms, starch is converted to glucose monosaccharide. This sugared starch was subjected to alcoholic fermentation. They obtained an C<sub>2</sub>H<sub>5</sub>OH yield of about 7.5 mg/mL (7500 ppm) with enzyme-mediated glycation followed by inactivated yeast fermentation. The unripe fruits did not release any C<sub>2</sub>H<sub>5</sub>OH; however, the ripe and over-ripe fruits of the Neotropical palm contained C<sub>2</sub>H<sub>5</sub>OH within



the pulp at average concentrations of 0.9% and 4.5% [105]. Fruit ripening was associated with significant changes in the color, sugar level, and  $C_2H_5OH$  content. However, the  $C_2H_5OH$  level required to detect spoilage of fruits and vegetable should be very low for early detection because the release of  $C_2H_5OH$  is due to the fermentation stage, which may occur after the ripening stage, which can be monitored by  $C_2H_4$  detection. As mentioned above, wasted or spoiled vegetables and fruits contain sugar since 80% of the bio  $C_2H_5OH$  is produced [106]. Thus,  $C_2H_5OH$  sensors are considered as important for the detection of spoilage of stored food. Thus, an ultra-sensitive  $C_2H_5OH$  sensor was developed based on highly defected CNTs [107]. The CNTs were fabricated by the PECVD method, as shown in Figure 4a. The sensor was operated at a low temperature of RT. It showed a response of 8.8% against an  $C_2H_5OH$  concentration of 50 ppm. Moreover, it demonstrated an LOD of 5 ppm with a high capability of detecting different concentrations, as shown in Figure 4b. Coulomb interaction was proposed as the sensing mechanism, considering the polarity nature of  $C_2H_5OH$  due to the hydroxyl group bonded to the carbon atom end, since the oxygen and hydrogen electronegativities are 3.44 and 2.2, respectively. Based on this truth, the physical adsorption of the  $C_2H_5OH$  molecules can create Coulomb force (electric dipole) between the CNTs and  $C_2H_5OH$ , as shown in Figure 4c.

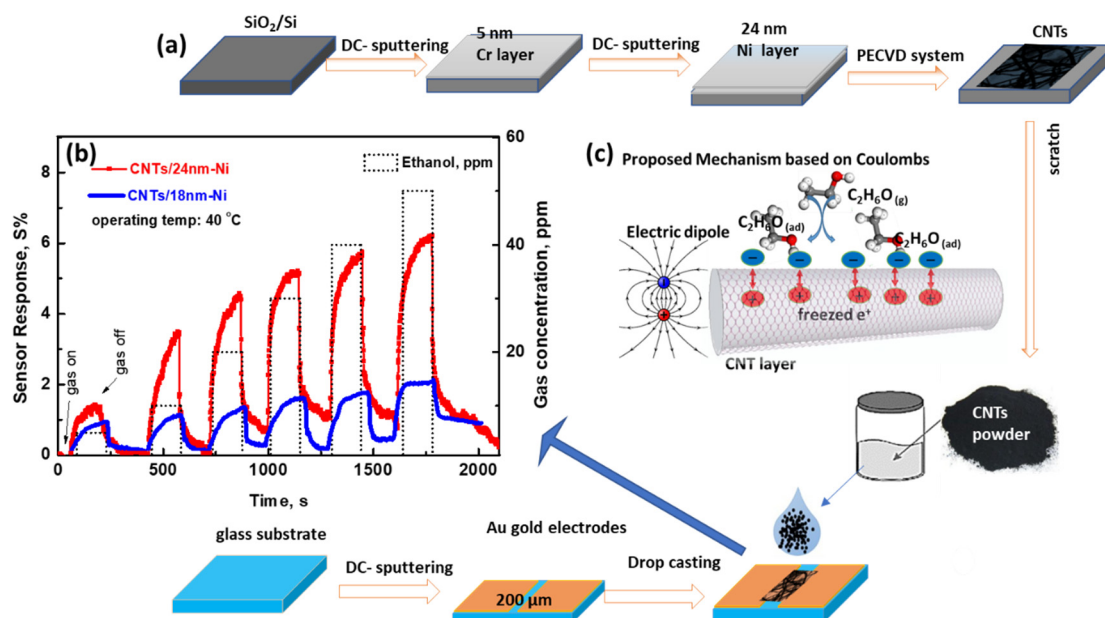


**Figure 4.** (a) Scheme of the synthesis of CNTs and sensing device fabrication; (b) signal as a function of time at different gas concentrations for the sensor prepared by 18 and 24 nm of Ni catalyst layer; and (c) the  $C_2H_5OH$  sensing mechanism. Figures reproduced with permission from [107].

As mentioned earlier, the use of hybrid sensing layers has a positive influence on the sensing properties (Table 5). Mono-oxides are still being developed by organic materials to meet the sensing requirements because of their ease of manufacture and low complexity. For example, regarding ZnO spheres assembled by porous nanosheets via a one-step hydrothermal method, their properties influence the  $C_2H_5OH$  gas sensing response by adjusting the amount of polyvinylpyrrolidone (PVP) [108]. A sensor based on a ZnO nanosphere compound manufactured by 3.3 g PVP achieved a response of ~58.4 to 100 ppm  $C_2H_5OH$  but was operated at high temperatures of 250 °C. It is worth noting that this response is about 9.4 times higher than that observed for the ZnO nanosheet layer fabricated without PVP. Moreover, the LOD can attain a ppb level, where a response of 1.17 was observed to an  $C_2H_5OH$  concentration of 500 ppb. However,  $In_2O_3$  nanotube composites derived from MOF and  $Cr_2O_3$  nanoparticles have been used as the sensing layer [109]. The  $In_2O_3/Cr_2O_3$  composite sensor showed an excellent performance in sensing  $C_2H_5OH$  at RT for a concentration as low as 5 ppm. It also showed excellent selectivity, good repeatability,

quick response/recovery time, and long-term stability. Additionally, Yu et al. [110] obtained hollow ZnSnO<sub>3</sub> microspheres decorated with CeO<sub>2</sub> nanoparticles with heterogeneous structures to meet the requirements for C<sub>2</sub>H<sub>5</sub>OH detection. The hollow microspheres of CeO<sub>2</sub>/ZnSnO<sub>3</sub> showed a response of 219.2 to 100 ppm of C<sub>2</sub>H<sub>5</sub>OH compared with pure ZnSnO<sub>3</sub>, which showed a much lower response. It also exhibited superior selectivity and a quick recovery response to C<sub>2</sub>H<sub>5</sub>OH compared to other gases. These properties of C<sub>2</sub>H<sub>5</sub>OH were explained by the large quantity of oxygen dissociation and the *n-n* hetero bonding of ZnSnO<sub>3</sub>/CeO<sub>2</sub>. Not only do the binary compounds show an optimal response to C<sub>2</sub>H<sub>5</sub>OH but the synthesis of a tri-compound, such as MoO<sub>2</sub>-Ni-graphene, sensing material also has attractive sensing properties [111]. By testing the gas sensing performance of this layer to C<sub>2</sub>H<sub>5</sub>OH, a significant improvement in the response of up to 105 was found when exposed to 1000 ppm at RT. The LOD at RT was 15 ppm. A great impact regarding the improvement of the sensing properties of C<sub>2</sub>H<sub>5</sub>OH was observed due to the metallic nature of Mo and Ni on the surface of graphene. This sensor has been tested for long periods and has enhanced its stability as a good candidate for the commercial market.

**Table 5.** The most recent chemiresistive C<sub>2</sub>H<sub>5</sub>OH sensors reported in the literature.

Sensor	Operating Temp. (°C)	C <sub>2</sub> H <sub>5</sub> OH Concentration	Response %	Limit of Detection	Ref.
MWCNTs	RT	50 ppm	8.8	5 ppm	[107]
ZnO microspheres	250	100 ppm	58.4	1.17 ppb	[108]
CeO <sub>2</sub> /ZnSnO <sub>3</sub>	200	100 ppm	219	0.5 ppm	[110]
In <sub>2</sub> O <sub>3</sub> /Cr <sub>2</sub> O <sub>3</sub>	RT	50 ppm	15.6	5 ppm	[109]
MoO <sub>2</sub> -Ni-Graphene	RT	1000 ppm	105	15 ppm	[111]
Ag/ZnO nano-generator	RT	800 ppm	88	10 ppm	[112]
TiO <sub>2</sub> @2D-TiC	RT	60 ppm	390	10 ppm	[113]
PEG/MWCNTs	RT	50 ppm	2.9	–	[114]
Au-CNFs	RT	100 ppm	6.3	50 ppm	[115]
High-density CNTs	RT	50 ppm	0.18	–	[116]

At the end of this section, we explain a good approach to sensor development. Interestingly, a self-powered sensor for C<sub>2</sub>H<sub>5</sub>OH was fabricated based on an Ag/ZnO nanowire array [112]. The self-power was served by the piezoelectric phenomena of the Ag/ZnO array. At the same time, it could sense the concentration of C<sub>2</sub>H<sub>5</sub>OH at RT by changing the piezoelectric output. The piezoelectric output was significantly increased by the addition of Ag. The piezoelectric voltage decreased from 1.7–0.2 V when the sensor was exposed to 10–1000 ppm of C<sub>2</sub>H<sub>5</sub>OH. The change in the output voltage was attributed to Ag, where Ag atoms play a catalytic role, in addition to the formation of Schottky barriers between Ag and ZnO. This sensor design provides an opportunity to achieve a self-powered gas sensor in various applications. Additionally, a promising sensor was fabricated by Raghu et al. [113]. They developed flexible sheets of TiO<sub>2</sub> grafted with 2D-TiC nanoparticles (TiO<sub>2</sub>@2DTiC) operating at RT. The flexible sensor showed high selectivity towards C<sub>2</sub>H<sub>5</sub>OH gas at a concentration of 10 ppb to 60 ppm. This was attributed to the availability of electron-hole synthesis at the TiO<sub>2</sub>/2D-TiC interfaces. This wearable sensor can be electronically printed for use in the environmental monitoring sectors of long-term stored foods.

#### 4. Future Perspectives and Conclusions

In summary, toxic gas sensors play an important role in food production and control. Therefore, researchers have recently devoted significant attention to various gas sensing materials to achieve high-performance gas sensors. However, knowledge of the aspects of the applications and the appropriateness of the environment in which the sensor is intended to be used may help a lot in the development of optimal sensors. The prospects for the use of sensor technology in food production and monitoring are: (1) Development of simple sensors that operate at low temperatures and preferably RT to save energy consumed during the monitoring process and the lifespan of the sensing material and accordingly, (2) the

development of reliable sensors that can be woven into the clothing of workers in meat and fish stores to identify their condition in real time; (3) the identification of promising candidates for reducing device circuit complexity, which can be integrated into portable devices with low-energy-density batteries; and (4) the design of high-precision sensors to monitor the strategic stock of foodstuffs, especially C<sub>2</sub>H<sub>4</sub> gas, to monitor the quality of stored fruits and vegetables and control their age. Chemiresistive sensors are easy to manufacture, cheap, and easy to integrate. It is noted that the most suitable sensing layers for these environments are those made of polymer and nanocarbon materials combined with oxides. Researchers are interested in obtaining improvements in the sensitivity, selectivity, limit of detection, and operating temperature using a new mixture of nanomaterials that display different shapes. However, challenges remain. Thus, we reported the use of gases in food production, processing, and monitoring to provide knowledge for the sensing community.

**Author Contributions:** Conceptualization, N.M.S., F.A., O.S. and S.K.; methodology, N.M.S., F.A., O.S. and S.K.; formal analysis, N.M.S., F.A., O.S. and S.K.; writing—original draft preparation, N.M.S. and F.A.; writing—review and editing, N.M.S., O.S. and S.K.; visualization, N.M.S.; supervision, N.M.S.; project administration, N.M.S.; funding acquisition, N.M.S. All authors have read and agreed to the published version of the manuscript.

**Funding:** This work was supported by the Deanship of Scientific Research, Vice Presidency for Graduate Studies and Scientific Research, King Faisal University, Saudi Arabia [Grant No. CHAIR60].

**Institutional Review Board Statement:** Not applicable.

**Informed Consent Statement:** Not applicable.

**Data Availability Statement:** Not applicable.

**Acknowledgments:** We extend our appreciation to the Deanship of Scientific Research, Vice Presidency for Graduate Studies and Scientific Research, King Faisal University, Saudi Arabia, for extending the grant to [Grant No. GRANT1379].

**Conflicts of Interest:** The authors declare no conflict of interest.

## References

1. Cozzolino, A.; Verona, G.; Rothaermel, F.T. Unpacking the Disruption Process: New Technology, Business Models, and Incumbent Adaptation. *J. Manag. Stud.* **2018**, *55*, 1166–1202. [CrossRef]
2. Blanco-Rojo, R.; Sandoval-Insausti, H.; López-García, E.; Graciani, A.; Ordovás, J.M.; Banegas, J.R.; Rodríguez-Artalejo, F.; Guallar-Castillón, P. Consumption of Ultra-Processed Foods and Mortality: A National Prospective Cohort in Spain. *Mayo Clin. Proc.* **2019**, *94*, 2178–2188. [CrossRef] [PubMed]
3. Rico-Campà, A.; Martínez-González, M.A.; Alvarez-Alvarez, I.; Mendonça, R.D.; de la Fuente-Arrillaga, C.; Gómez-Donoso, C.; Bes-Rastrollo, M. Association between consumption of ultra-processed foods and all cause mortality: SUN prospective cohort study. *BMJ* **2019**, *365*, 11949. [CrossRef]
4. Fletcher, B.; Mullane, K.; Platts, P.; Todd, E.; Power, A.; Roberts, J.; Chapman, J.; Cozzolino, D.; Chandra, S. Advances in meat spoilage detection: A short focus on rapid methods and technologies. *CYTA—J. Food.* **2018**, *16*, 1037–1044. [CrossRef]
5. World Health Organization (WHO). Draft WHO Global Strategy for Food Safety 2022–2030. Available online: <https://www.who.int/publications/m/item/draft-who-global-strategy-for-food-safety-2022-2030> (accessed on 15 August 2022).
6. Google Scholar. h5-index in Food Science and Technology. 2022. Available online: [https://scholar.google.com/citations?view\\_op=top\\_venues&hl=en&vq=bio\\_foodsciencetechnology](https://scholar.google.com/citations?view_op=top_venues&hl=en&vq=bio_foodsciencetechnology) (accessed on 15 August 2022).
7. Report Overview: Gas Sensor Market Size, Share & Trends Analysis Report by Product, by Type, by Technology, by End Use, by Region, and Segment Forecasts, 2022–2030. 2022. Available online: <https://www.grandviewresearch.com/industry-analysis/gas-sensors-market> (accessed on 15 August 2022).
8. Djenane, D.; Roncalés, P. Carbon monoxide in meat and fish packaging: Advantages and limits. *Foods* **2018**, *7*, 12. [CrossRef] [PubMed]
9. Cameron, A.C.; Talasila, P.C.; Joles, D.W. Predicting Film Permeability Needs for Modified-atmosphere Packaging of Lightly Processed Fruits and Vegetables. *HortScience* **2019**, *30*, 25–34. [CrossRef]
10. Odunlami, O.A.; Abatan, O.G.; Busari, A.A.; Alao, G.T.; Elehinafe, F.B.; Emekekwe, C.O. Assessment of hydrogen sulfide emission levels on the floors of some selected bakeries in southwestern Nigeria. *IOP Conf. Ser. Mater. Sci. Eng.* **2021**, *1036*, 012067. [CrossRef]
11. Guido, L.F. Sulfites in beer: Reviewing regulation, analysis and role. *Sci. Agric.* **2016**, *73*, 189–197. [CrossRef]

12. Aissa, K.A.; Zheng, J.L.; Estel, L. Thermal Stability of Epoxidized and Carbonated Vegetable Oils. *Org. Process Res. Dev.* **2016**, *20*, 948–953. [CrossRef]
13. Fernandez, C.M.; Alves, J.; Gaspar, P.D.; Lima, T.M.; Silva, P.D. Innovative processes in smart packaging. A systematic review. *J. Sci. Food Agric.* **2022**. [CrossRef]
14. Nguyen, L.H.; Naficy, S.; McConchie, R.; Dehghani, F.; Chandrawati, R. Polydiacetylene-based sensors to detect food spoilage at low temperatures. *J. Mater. Chem. C* **2019**, *7*, 1919–1926. [CrossRef]
15. Shaalan, N.M.; Ahmed, F.; Kumar, S.; Melaibari, A.; Hasan, P.M.Z.; Aljaafari, A. Monitoring Food Spoilage Based on a Defect-Induced Multiwall Carbon Nanotube Sensor at Room Temperature: Preventing Food Waste. *ACS Omega* **2020**, *5*, 30531–30537. [CrossRef] [PubMed]
16. Xiao, Y.Y.; Kuang, J.F.; Qi, X.N.; Ye, Y.J.; Wu, Z.X.; Chen, J.Y.; Lu, W.J. A comprehensive investigation of starch degradation process and identification of a transcriptional activator MabHLH6 during banana fruit ripening. *Plant Biotechnol. J.* **2018**, *16*, 151–164. [CrossRef] [PubMed]
17. Atkinson, S.; Algers, B.; Pallisera, J.; Velarde, A.; Llonch, P. Animal Welfare and Meat Quality Assessment in Gas Stunning during Commercial Slaughter of Pigs Using Acute Hypercapnia (90 % CO<sub>2</sub> in Air). *Animals* **2020**, *12*, 2440. [CrossRef]
18. Ehret, G.; Amediak, A.; Fix, A.; Kiemle, C.; Quatrevalet, M.; Wirth, M.; Wolff, S. *Active Remote Sensing of the Greenhouses Gases CO<sub>2</sub> and CH<sub>4</sub> with CHARM-F on the HALO aircraft*. AGU Fall Meeting Abstracts; SAO/NASA: Washington, DC, USA, 2019; p. A51M-2727.
19. Notarnicola, B.; Tassielli, G.; Alexander, P.; Monforti, F. Energy flows and greenhouses gases of EU (European Union) national breads using an LCA (Life Cycle Assessment) approach. *J. Clean. Prod.* **2017**, *140*, 455–469. [CrossRef]
20. Shaalan, N.M.; Morsy, A.E.A.; Abdel-Rahim, M.A.; Rashad, M. Simple preparation of Ni/CuO nanocomposites with superior sensing activity toward the detection of methane gas. *Appl. Phys. A Mater. Sci. Process.* **2021**, *127*, 455. [CrossRef]
21. Shaalan, N.M.; Saber, O.; Ahmed, F.; Aljaafari, A.; Kumar, S. Growth of defect-induced carbon nanotubes for low-temperature fruit monitoring sensor. *Chemosensors* **2021**, *9*, 131. [CrossRef]
22. Adley, C.C. Past, Present and Future of Sensors in Food Production. *Foods* **2014**, *3*, 491–510. [CrossRef]
23. Zaki, S.A.; Abd-Elrahman, M.I.; Abu-Sehly, A.A.; Almokhtar, M.; Soltan, A.S.; Shaalan, N.M. Solar cell fabrication from semiconducting binary tin sulfide alloy on Si substrate. *Sol. Energy* **2021**, *228*, 206–215. [CrossRef]
24. Shaalan, N.M.; Hamad, D. Low-Temperature Hydrogen Sensor Based on Sputtered Tin Dioxide Nanostructures through Slow Deposition Rate. *Appl. Surf. Sci.* **2022**, *598*, 153857. [CrossRef]
25. Kamble, P.; Jadhav, B.T. Quality Parameters of Wine: A Review in Grams. *Int. J. Eng. Appl. Sci. Technol.* **2021**, *6*, 177–182.
26. Silva, M.M.; Lidon, F.C. Food preservatives—An overview on applications and side effects. *Emirates J. Food Agric.* **2016**, *28*, 366–373. [CrossRef]
27. Black, C.M.; Chu, A.J.; Thomas, G.H.; Routledge, A.; Duhme-Klair, A.-K. Synthesis and antimicrobial activity of an SO<sub>2</sub>-releasing siderophore conjugate. *J. Inorg. Biochem.* **2022**, *234*, 111875. [CrossRef] [PubMed]
28. Howe, P.A.; Worobo, R.; Sacks, G.L. Conventional Measurements of Sulfur Dioxide (SO<sub>2</sub>) in Red Wine Overestimate SO<sub>2</sub> Antimicrobial Activity. *Am. J. Enol. Vitic.* **2018**, *69*, 210–220. [CrossRef]
29. Chen, Y.; Zeng, W.; Fang, F.; Yu, S.; Zhou, J. Elimination of ethyl carbamate in fermented foods. *Food Biosci.* **2022**, *47*, 101725. [CrossRef]
30. Jongman, E.C.; Woodhouse, R.; Rice, M.; Rault, J.L. Pre-slaughter factors linked to variation in responses to carbon dioxide gas stunning in pig abattoirs. *Animal* **2021**, *15*, 100134. [CrossRef] [PubMed]
31. Spizzica, A. Animal production: Anesthesia of pigs and poultry before slaughter. In *Gases in Agro-Food Processes*; Cachon, R., Girardon, P., Voilley, A., Eds.; Academic Press: Cambridge, MA, USA, 2019; pp. 127–151. [CrossRef]
32. Bao, J.; Lu, W.-H.; Zhao, J.; Bi, X.T. Greenhouses for CO<sub>2</sub> sequestration from atmosphere. *Carbon Resour. Convers.* **2018**, *1*, 183–190. [CrossRef]
33. Goldammer, T. *Greenhouse Management: A Guide to Operations and Technology*, 1st ed.; Apex Publishing: Clacton-on-Sea, Essex, UK, 2019.
34. Frantz, J.M. Elevating Carbon Dioxide in a Commercial Greenhouse Reduced Overall Fuel Carbon Consumption and Production Cost When Used in Combination with Cool Temperatures for Lettuce Production. *HorTechnology* **2011**, *21*, 647–651. [CrossRef]
35. Blom, T.J.; Straver, W.A.; Ingratta, F.J.; Khosla, S.S.K.; Brown, W. Carbon Dioxide in Greenhouses, Ontario. 2022. Available online: <http://omafra.gov.on.ca/english/crops/facts/00-077.htm> (accessed on 2 July 2022).
36. Kokila, V.; Prasanna, R.; Kumar, A.; Nishanth, S.; Shukla, J.; Gulia, U.; Nain, L.; Shivay, Y.S.; Singh, A.K. Cyanobacterial inoculation in elevated CO<sub>2</sub> environment stimulates soil C enrichment and plant growth of tomato. *Environ. Technol. Innov.* **2022**, *26*, 102234. [CrossRef]
37. Santhanam, N.N.; Ahamed, K.S.V. Greenhouse Gas Sensors Fabricated with New Materials for Climatic Usage: A Review. *ChemEngineering* **2018**, *2*, 38. [CrossRef]
38. Maske, V.R.; Dhulap, V.P. Development of Handy Prototype Gas Sensors Kit for Monitoring of Ambient Green House Gases from Solid Waste Disposal Sites of Solapur City. *AIP Conf. Proc.* **2018**, *1989*, 020024. [CrossRef]
39. Qu, P.; Zhang, M.; Fan, K.; Guo, Z. Microporous modified atmosphere packaging to extend shelf life of fresh foods: A review. *Crit. Rev. Food Sci. Nutr.* **2022**, *62*, 51–65. [CrossRef] [PubMed]



40. Li, Y.; Zhou, C.; He, J.; Wu, Z.; Sun, Y.; Pan, D.; Tian, H.; Xia, Q. Combining e-beam irradiation and modified atmosphere packaging as a preservation strategy to improve physicochemical and microbiological properties of sauced duck product. *Food Control*. **2022**, *136*, 108889. [CrossRef]
41. Wang, Q.; Chen, Q.; Xu, J.; Sun, F.; Liu, H.; Kong, B. Effects of Modified Atmosphere Packaging with Various CO<sub>2</sub> Concentrations on the Bacterial Community and Shelf-Life of Smoked Chicken Legs. *Foods* **2022**, *11*, 559. [CrossRef]
42. McNulty, R.; Kuchi, N.; Xu, E.; Gunja, N. Food-induced methemoglobinemia: A systematic review. *J. Food Sci.* **2022**, *87*, 1423–1448. [CrossRef]
43. Zhao, Q.; Hazarika, A.; Chen, X.; Harvey, S.P.; Larson, B.W.; Teeter, G.R.; Liu, J.; Song, T.; Xiao, C.; Shaw, L.; et al. High efficiency perovskite quantum dot solar cells with charge separating heterostructure. *Nat. Commun.* **2019**, *10*, 2842. [CrossRef]
44. Aslam, A.; Mughal, T.A. A Review on Microalgae to Achieve Maximal Carbon Dioxide (CO<sub>2</sub>) Mitigation from Industrial Flue Gases. *Int. J. Res. Advent Technol.* **2016**, *4*, 2321–9637.
45. Iglina, T.; Iglina, P.; Pashchenko, D. Industrial CO<sub>2</sub> Capture by Algae: A Review and Recent Advances. *Sustainability* **2022**, *14*, 3801. [CrossRef]
46. Onyeaka, H.; Miri, T.; Obileke, K.; Hart, A.; Anumudu, C.; Al-sharif, Z.T. Minimizing carbon footprint via microalgae as a biological capture. *Carbon Capture Sci. Technol.* **2021**, *1*, 100007. [CrossRef]
47. Singh, J.; Dhar, D.W. Overview of Carbon Capture Technology: Microalgal Biorefinery Concept and State-of-the-Art. *Front. Mar. Sci.* **2019**, *6*, 29. [CrossRef]
48. Nastiti, P.W.; Bintoro, N. Classification of Freshness Levels and Prediction of Changes in Evolution of NH<sub>3</sub> and H<sub>2</sub>S Gases from Chicken Meat during Storage at Room Temperature. *J. Agric. Eng.* **2022**, *11*, 90–98. [CrossRef]
49. Zhang, Y.; Lim, L.T. Colorimetric array indicator for NH<sub>3</sub> and CO<sub>2</sub> detection. *Sens. Actuators B Chem.* **2018**, *255*, 3216–3226. [CrossRef]
50. Edita, R.; Darius, G.; Vinauskienė, R.; Eisinaite, V.; Balčiūnas, G.; Dobilienė, J.; Tamkutė, L. Rapid evaluation of fresh chicken meat quality by electronic nose. *Czech J. Food Sci.* **2018**, *36*, 420–426. [CrossRef]
51. Matindoust, S.; Farzi, G.; Nejad, M.B.; Shahrokhbadi, M.H. Polymer-based gas sensors to detect meat spoilage: A review, *React. Funct. Polym.* **2021**, *165*, 104962. [CrossRef]
52. Orono, M. Controlled Atmosphere Storage. 2022. Available online: <https://extension.umaine.edu/fruit/harvest-and-storage-of-tree-fruits/controlled-atmosphere-storage/> (accessed on 22 May 2022).
53. Krupa, T.; Tomala, K. Effect of oxygen and carbon dioxide concentration on the quality of minikiwi fruits after storage. *Agronomy* **2021**, *11*, 2251. [CrossRef]
54. Erkan, M.; Dogan, A. *Controlled and Modified Atmospheres for Fresh and Fresh-Cut Produce*, In *Subtropical Fruits: Pomegranates*; Academic Press: Amsterdam, The Netherlands, 2020; Chapter 18.11; pp. 477–486. [CrossRef]
55. Tadiello, A.; Ziosi, V.; Negri, A.S.; Noferini, M.; Fiori, G.; Busatto, N.; Espen, L.; Costa, G.; Trainotti, L. On the role of ethylene, auxin and a GOLVEN-like peptide hormone in the regulation of peach ripening. *BMC Plant Biol.* **2016**, *16*, 1–17. [CrossRef]
56. Iqbal, N.; Khan, N.A.; Ferrante, A.; Trivellini, A.; Francini, A.; Khan, M.I.R. Ethylene role in plant growth, development and senescence: Interaction with other phytohormones. *Front. Plant Sci.* **2017**, *8*, 1–19. [CrossRef]
57. Thompson, A.K. *Controlled Atmosphere Storage of Fruits and Vegetables*, 2nd ed.; CABI Publishing: Wallington, UK, 2010.
58. Fong, D.; Luo, S.X.; Andre, R.S.; Swager, T.M. Trace Ethylene Sensing via Wacker Oxidation. *ACS Cent. Sci.* **2020**, *6*, 507–512. [CrossRef]
59. Li, Y.; Hodak, M.; Lu, W.; Bernholc, J. Selective sensing of ethylene and glucose using carbon-nanotube-based sensors: An ab initio investigation. *Nanoscale* **2017**, *9*, 1687–1698. [CrossRef]
60. Kathirvelan, J.; Vijayaraghavan, R. An infrared based sensor system for the detection of ethylene for the discrimination of fruit ripening. *Infrared Phys. Technol.* **2017**, *85*, 403–409. [CrossRef]
61. Zhao, Q.; Duan, Z.; Yuan, Z.; Li, X.; Wang, S.; Liu, B.; Zhang, Y.; Jiang, Y.; Tai, H. High performance ethylene sensor based on palladium-loaded tin oxide: Application in fruit quality detection. *Chin. Chem. Lett.* **2020**, *31*, 2045–2049. [CrossRef]
62. Pattanauwat, P.; Aht-Ong, D. In-Situ Electrochemical Synthesis of Novel Sensitive Layer of Polyaniline/Multiwall Carbon Nanotube/Tin Oxide Hybrid Materials for Ethylene Gas Detection. *Polym. Plast. Technol. Eng.* **2013**, *52*, 189–194. [CrossRef]
63. Li, B.; Li, M.; Meng, F.; Liu, J. Chemical Highly sensitive ethylene sensors using Pd nanoparticles and rGO modified flower-like hierarchical porous  $\alpha$ -Fe<sub>2</sub>O<sub>3</sub>. *Sens. Actuators B* **2019**, *290*, 396–405. [CrossRef]
64. Jeong, S.Y.; Moon, Y.K.; Kim, T.H.; Park, S.W.; Kim, K.B.; Kang, Y.C.; Lee, J.H. A New Strategy for Detecting Plant Hormone Ethylene Using Oxide Semiconductor Chemiresistors: Exceptional Gas Selectivity and Response Tailored by Nanoscale Cr<sub>2</sub>O<sub>3</sub> Catalytic Overlay. *Adv. Sci.* **2020**, *7*, 1903093. [CrossRef] [PubMed]
65. Barreca, D.; Gasparotto, A.; Gri, F.; Comini, E.; Maccato, C. Plasma-Assisted Growth of  $\beta$ -MnO<sub>2</sub> Nanosystems as Gas Sensors for Safety and Food Industry Applications. *Adv. Mater. Interfaces.* **2018**, *5*, 1800792. [CrossRef]
66. Sholehah, A.; Karmala, K.; Huda, N.; Utari, L.; Septiani, N.L.W.; Yulianto, B. Structural effect of ZnO-Ag chemoresistive sensor on flexible substrate for ethylene gas detection. *Sens. Actuators A Phys.* **2021**, *331*, 112934. [CrossRef]
67. Food Science Australia. *Assessing Meat Quality after Ammonia Leaks*; Food Science Australia: Cherrybrook, NSW, Australia, 2002.
68. Zhang, Y.; Zhang, J.; Jiang, Y.; Duan, Z.; Liu, B.; Zhao, Q.; Wang, S.; Yuan, Z.; Tai, H. Ultrasensitive flexible NH<sub>3</sub> gas sensor based on polyaniline/SrGe<sub>4</sub>O<sub>9</sub> nanocomposite with ppt-level detection ability at room temperature. *Sens. Actuators B Chem.* **2020**, *319*, 128293. [CrossRef]



69. Mougkogiannis, P.; Turner, M.; Persaud, K. Amine Detection Using Organic Field Effect Transistor Gas Sensors. *Sensors* **2021**, *21*, 13. [CrossRef]
70. Rahmanudin, A.; Tate, D.J.; Marcial-Hernandez, R.; Bull, N.; Garlapati, S.K.; Zamhuri, A.; Khan, R.U.; Faraji, S.; Gollu, S.R.; Persaud, K.C.; et al. Robust High-Capacitance Polymer Gate Dielectrics for Stable Low-Voltage Organic Field-Effect Transistor Sensors. *Adv. Electron. Mater.* **2020**, *6*, 1901127. [CrossRef]
71. Li, P.; Wang, B.; Qin, C.; Han, C.; Sun, L.; Wang, Y. Band-gap-tunable CeO<sub>2</sub> nanoparticles for room-temperature NH<sub>3</sub> gas sensors. *Ceram. Int.* **2020**, *46*, 19232–19240. [CrossRef]
72. Andre, R.S.; Shimizu, F.M.; Miyazaki, C.M.; Riul, A.; Manzani, D.; Ribeiro, S.J.L.; Oliveira, O.N.; Mattoso, L.H.C.; Correa, D.S. Hybrid layer-by-layer (LbL) films of polyaniline, graphene oxide and zinc oxide to detect ammonia. *Sens. Actuators B Chem.* **2017**, *238*, 795–801. [CrossRef]
73. Lee, S.H.; Eom, W.; Shin, H.; Ambade, R.B.; Bang, J.H.; Kim, H.W.; Han, T.H. Room-Temperature, Highly Durable Ti<sub>3</sub>C<sub>2</sub>T<sub>x</sub> MXene/Graphene Hybrid Fibers for NH<sub>3</sub> Gas Sensing. *ACS Appl. Mater. Interfaces* **2020**, *12*, 10434–10442. [CrossRef] [PubMed]
74. Goswami, P.; Gupta, G. Recent progress of flexible NO<sub>2</sub> and NH<sub>3</sub> gas sensors based on transition metal dichalcogenides for room temperature sensing. *Mater. Today Chem.* **2022**, *23*, 100726. [CrossRef]
75. Fernández-Ramos, M.D.; Capitán-Vallvey, L.F.; Pastrana-Martínez, L.M.; Morales-Torres, S.; Maldonado-Hódar, F.J. Chemical Chemoresistive NH<sub>3</sub> gas sensor at room temperature based on the carbon. *Sens. Actuators B Chem.* **2022**, *368*, 132103. [CrossRef]
76. Han, D.; Han, X.; Zhang, X.; Wang, W.; Li, D.; Li, H.; Sang, S. Highly sensitive and rapidly responding room-temperature NH<sub>3</sub> gas sensor that is based on exfoliated black phosphorus. *Sens. Actuators B Chem.* **2022**, *367*, 132038. [CrossRef]
77. Wu, K.; Debligny, M.; Zhang, C. Room temperature gas sensors based on Ce doped TiO<sub>2</sub> nanocrystals for highly sensitive NH<sub>3</sub> detection. *Chem. Eng. J.* **2022**, *444*, 136449. [CrossRef]
78. Majumder, D.; Roy, S. ScienceDirect Room Temperature Synthesis of TiO<sub>2</sub> Nanospheres: Ammonia Sensing Characteristics. *Mater. Today Proc.* **2018**, *5*, 9811–9816. [CrossRef]
79. Zhou, Y.; Wang, Y.; Wang, Y.; Yu, H.; Zhang, R.; Li, J.; Zang, Z.; Li, X. MXene Ti<sub>3</sub>C<sub>2</sub>T<sub>x</sub>-Derived Nitrogen-Functionalized Heterophase TiO<sub>2</sub> Homo Junctions for Room-Temperature Trace Ammonia Gas Sensing. *ACS Appl. Mater. Interfaces.* **2021**, *13*, 56485–56497. [CrossRef]
80. Tai, H.; Duan, Z.; He, Z.; Li, X.; Xu, J.; Liu, B.; Jiang, Y. Enhanced ammonia response of Ti<sub>3</sub>C<sub>2</sub>T<sub>x</sub> nanosheets supported by TiO<sub>2</sub> nanoparticles at room temperature. *Sens. Actuators B Chem.* **2019**, *298*, 126874. [CrossRef]
81. Guerrero, R.F.; Cantos-Villar, E. Demonstrating the efficiency of sulphur dioxide replacements in wine: A parameter review. *Trends Food Sci. Tech.* **2015**, *42*, 27–43. [CrossRef]
82. New Jersey Department of Health. *Hazardous Substance Fact Sheet: Sulfur Dioxide*; New Jersey Department of Health: Clifton, NJ, USA, 2010.
83. Liu, L.; Zhou, P.; Su, X.; Liu, Y.; Sun, Y.; Yang, H.; Fu, H.; Qu, X.; Liu, S.; Zheng, S. Synergistic Ni single atoms and oxygen vacancies on SnO<sub>2</sub> nanorods toward promoting SO<sub>2</sub> gas sensing. *Sens. Actuators B Chem.* **2022**, *351*, 130983. [CrossRef]
84. Shinde, R.B.; Padalkar, N.S.; Sadavar, S.V.; Kale, S.B.; Magdum, V.V.; Chitare, Y.M.; Kulkarni, S.P.; Patil, U.M.; Parale, V.G.; Park, H.H.; et al. 2D–2D lattice engineering route for intimately coupled nanohybrids of layered double hydroxide and potassium hexaniobate: Chemiresistive SO<sub>2</sub> sensor. *J. Hazard. Mater.* **2022**, *432*, 128734. [CrossRef] [PubMed]
85. Hsiao, Y.-J.; Shi, Z.-H.; Nagarjuna, Y.; Huang, Z.-Y.; Lai, T.-Y.; Wu, S. Double-Layered NiO/SnO<sub>2</sub> Sensor for Improved SO<sub>2</sub> Gas Sensing with MEMS Microheater Device. *ECS J. Solid State Sci. Technol.* **2022**, *11*, 57002. [CrossRef]
86. Hsueh, T.-J.; Lee, S.-H. A La<sub>2</sub>O<sub>3</sub> Nanoparticle SO<sub>2</sub> Gas Sensor that Uses a ZnO Thin Film and Au Adsorption. *J. Electrochem. Soc.* **2021**, *168*, 77507. [CrossRef]
87. Aranthady, C.; Jangid, T.; Gupta, K.; Mishra, A.K.; Kaushik, S.D.; Siruguri, V.; Rao, G.M.; Shanbhag, G.V.; Sundaram, N.G. Selective SO<sub>2</sub> detection at low concentration by Ca substituted LaFeO<sub>3</sub> chemiresistive gas sensor: A comparative study of LaFeO<sub>3</sub> pellet vs thin film. *Sens. Actuators B Chem.* **2021**, *329*, 129211. [CrossRef]
88. Jha, R.K.; Nanda, A.; Bhat, N. Sub-ppm sulfur dioxide detection using MoS<sub>2</sub> modified multi-wall carbon nanotubes at room temperature. *Nano Sel.* **2022**, *3*, 98–107. [CrossRef]
89. Zhai, Z.; Zhang, X.; Wang, J.; Li, H.; Sun, Y.; Hao, X.; Qin, Y.; Niu, B.; Li, C. Washable and flexible gas sensor based on UiO-66-NH<sub>2</sub> nanofibers membrane for highly detecting SO<sub>2</sub>. *Chem. Eng. J.* **2022**, *428*, 131720. [CrossRef]
90. Ingle, N.; Sayyad, P.; Deshmukh, M.; Bodkhe, G.; Mahadik, M.; Al-Gahouari, T.; Shirsat, S.; Shirsat, M.D. A chemiresistive gas sensor for sensitive detection of SO<sub>2</sub> employing Ni-MOF modified –OH-SWNTs and –OH-MWNTs. *Appl. Phys. A Mater. Sci. Process.* **2021**, *127*, 1–10. [CrossRef]
91. Thangamani, G.J.; Pasha, S.K.K. Titanium dioxide (TiO<sub>2</sub>) nanoparticles reinforced polyvinyl formal (PVF) nanocomposites as chemiresistive gas sensor for sulfur dioxide (SO<sub>2</sub>) monitoring. *Chemosphere* **2021**, *275*, 129960. [CrossRef]
92. Thomas, T.; Kumar, Y.; Alberto, J.; Ram, R.; Sepúlveda, S. Porous silicon/ $\alpha$ -MoO<sub>3</sub> nanohybrid based fast and highly sensitive CO<sub>2</sub> gas sensors. *Vacuum* **2021**, *184*, 109983. [CrossRef]
93. Bag, S.; Pal, K. Chemical Sulfonated poly (ether ether ketone) based carbon dioxide gas sensor: Impact of sulfonation degree on sensing behavior at different humid condition. *Sens. Actuators B Chem.* **2020**, *303*, 127115. [CrossRef]
94. Bouachma, S.; Ayouz-Chebout, K.; Kechouane, M.; Manseri, A.; Yaddadene, C.; Menari, H.; Gabouze, N. Synthesis of PSi-n-CuO-p-Cu<sub>2</sub>O-n heterostructure. *Appl. Phys. A Mater. Sci. Process.* **2022**, *128*, 69. [CrossRef]

95. Gupta, M.; Hawari, H.F.; Kumar, P. Copper Oxide/Functionalized Graphene Hybrid Nanostructures for Room Temperature Gas Sensing Applications. *Crystals* **2022**, *12*, 264. [[CrossRef](#)]
96. Lee, Z.Y.; Hawari, H.F.; Djaswadi, G.W.; Kamarudin, K. A Highly Sensitive Room Temperature CO<sub>2</sub> Gas Sensor Based on SnO<sub>2</sub>-rGO Hybrid Composite. *Materials* **2021**, *14*, 522. [[CrossRef](#)] [[PubMed](#)]
97. Amarnath, M.; Gurunathan, K. Highly selective CO<sub>2</sub> gas sensor using stabilized NiO-In<sub>2</sub>O<sub>3</sub> nanospheres coated reduced graphene oxide sensing electrodes at room temperature. *J. Alloys Compd.* **2021**, *857*, 157584. [[CrossRef](#)]
98. Nasirian, S. Applied Surface Science Enhanced carbon dioxide sensing performance of polyaniline/tin dioxide nanocomposite by ultraviolet light illumination. *Appl. Surf. Sci.* **2020**, *502*, 144302. [[CrossRef](#)]
99. Oh, W.; Liu, Y.; Sagadevan, S.; Fatema, K.N. Polymer bonded Graphene-LaNiSbWO<sub>4</sub> sensing performance under normal temperature condition. *Inorg. Nano-Metal Chem.* **2021**, *51*, 1803–1812. [[CrossRef](#)]
100. Kumar, U.; Yadav, B.C.; Haldar, T.; Dixit, C.K.; Kumar, P. Synthesis of MWCNT/PPY nanocomposite using oxidation polymerization method and its employment in sensing such as CO<sub>2</sub> and humidity. *J. Taiwan Inst. Chem. Eng.* **2020**, *113*, 419–427. [[CrossRef](#)]
101. Ghosh, A.; Zhang, C.; Zhang, H.; Shi, S. CO<sub>2</sub> Sensing Behavior of Calcium-Doped ZnO Thin Film: A Study to Address the Cross-Sensitivity of CO<sub>2</sub> in H<sub>2</sub> and CO Environment. *Langmuir* **2019**, *35*, 10267–10275. [[CrossRef](#)]
102. Roy, N.; Sinha, R.; Daniel, T.T.; Nemade, H.B.; Mandal, T.K. Highly Sensitive Room Temperature CO Gas Sensor Based on MWCNT-PDDA Composite. *IEEE Sens. J.* **2020**, *20*, 13245–13252. [[CrossRef](#)]
103. Nasresfahani, S.; Zargarpour, Z.; Sheikhi, M.H.; Ana, S.F.N. Improvement of the carbon monoxide gas sensing properties of polyaniline in the presence of gold nanoparticles at room temperature. *Synth. Met.* **2020**, *265*, 116404. [[CrossRef](#)]
104. SatishBabu, R.; Rentala, S.; Narsu, M.L.; Prameeladevi, Y.; Rao, D.G. Studies on ethanol production from spoiled starch rich vegetables by sequential batch fermentation. *Int. J. Biotechnol. Biochem.* **2010**, *6*, 351–358.
105. Dudley, R. Ethanol, fruit ripening, and the historical origins of human alcoholism in primate frugivory. *Integr. Comp. Biol.* **2004**, *44*, 315–323. [[CrossRef](#)] [[PubMed](#)]
106. Verma, M.; Mishra, V. Utilization of Fruit-Vegetable Waste as Lignocellulosic Feedstocks for Bioethanol Fermentation. In *Food Waste to Green Fuel: Trend & Development*; Srivastava, N., Malik, M.A., Eds.; Springer Nature: Singapore, 2022; pp. 189–211. [[CrossRef](#)]
107. Shaalan, N.M.; Ahmed, F.; Rashad, M.; Saber, O.; Kumar, S.; Aljaafari, A.; Ashoabi, A.; Mahmoud, A.Z.; Ezzeldien, M. Low-Temperature Ethanol Sensor via Defective Multiwalled Carbon Nanotubes. *Materials* **2022**, *15*, 4439. [[CrossRef](#)]
108. Jiang, B.; Lu, J.; Han, W.; Sun, Y.; Wang, Y.; Cheng, P.; Zhang, H.; Wang, C.; Lu, G. Chemical Hierarchical mesoporous zinc oxide microspheres for ethanol gas sensor. *Sens. Actuators B. Chem.* **2022**, *357*, 131333. [[CrossRef](#)]
109. Zhang, S.; Lin, Z.; Song, P.; Sun, J.; Wang, Q. MOF-derived In<sub>2</sub>O<sub>3</sub> nanotubes/Cr<sub>2</sub>O nanoparticles composites for superior ethanol gas-sensing performance at room temperature. *Ceram. Int.* **2022**, *48*, 28334–28342. [[CrossRef](#)]
110. Yu, S.; Jia, X.; Yang, J.; Wang, S.; Li, Y.; Song, H. Highly sensitive and low detection limit of ethanol gas sensor based on CeO<sub>2</sub> nanodot-decorated ZnSnO<sub>3</sub> hollow microspheres. *Ceram. Int.* **2022**, *48*, 14865–14875. [[CrossRef](#)]
111. Mehmood, S.; Zhao, X.; Fahad, M.; Ullah, F. MoO<sub>2</sub>-Ni-graphene ternary nanocomposite for a high-performance room-temperature ethanol gas sensor. *Appl. Surf. Sci.* **2021**, *554*, 149595. [[CrossRef](#)]
112. Zhang, X.; Wang, W.; Zhang, D. Self-powered ethanol gas sensor based on the piezoelectric Ag/ZnO nanowire arrays at room temperature. *J. Mater. Sci. Mater. Electron.* **2021**, *32*, 7739–7750. [[CrossRef](#)]
113. Raghu, A.V.; Karuppanan, K.K.; Nampoothiri, J.; Pullithadathil, B. Wearable, Flexible Ethanol Gas Sensor Based on TiO<sub>2</sub> Nanoparticles-Grafted 2D-Titanium Carbide Nanosheets. *ACS Appl. Nano Mater.* **2019**, *2*, 1152–1163. [[CrossRef](#)]
114. Liu, Z.; Yang, T.; Dong, Y.; Wang, X. A room temperature VOCs gas sensor based on a layer by layer multi-walled carbon nanotubes/poly-ethylene glycol composite. *Sensors* **2018**, *18*, 3113. [[CrossRef](#)] [[PubMed](#)]
115. Shoostari, M.; Sacco, L.N.; van Ginkel, J.; Vollebregt, S.; Salehi, A. Enhancement of Room Temperature Ethanol Sensing by Optimizing the Density of Vertically Aligned Carbon Nanofibers Decorated with Gold Nanoparticles. *Materials* **2022**, *15*, 1383. [[CrossRef](#)] [[PubMed](#)]
116. Young, S.J.; Lin, Z.D. Ethanol gas sensors based on multi-wall carbon nanotubes on oxidized Si substrate. *Microsyst. Technol.* **2018**, *24*, 55–58. [[CrossRef](#)]